ppGpp Is Present in and Functions to Regulate Sleep in Drosophila

Way Young,[1] Xiaohui Zhang,[2] Huimin Daixi,[1] Enxing Zhou,[1] Ying Liu,[2] Tao Wang,[1] Wenxia Zhang,[1] Xinxiang Zhang,[3] and Yi Rao[1,4,*]

[1]Capital Medical University, PKU-IDG/McGovern Institute for Brain Research, Peking-Tsinghua Center for Life Sciences, Peking University School of Life Sciences, and Chinese Institute for Brain Research, Beijing, Beijing, China.

[2]State Key Laboratory of Natural and Biomimetic Drugs, Peking University, 38 Xueyuan Road, Beijing 100191, China.

[3]College of Chemistry and Molecular Engineering, Peking University, Beijing, China

[4]Lead Contact

*Correspondence (email: yrao@pku.edu.cn)

SUMMARY

Discovery of molecules in living systems and demonstration of their functional roles are pivotal in furthering our understanding of the molecular basis of biology. ppGpp (guanosine-5'-diphosphate, 3'-diphosphate) has been detected in prokaryotes for more than five decades. Here we report that a genetic screen followed by chemical analysis revealed the presence of ppGpp in Drosophila. It can be detected in germ-free Drosophila and its level is controlled by an enzyme encoded by the *mesh1* gene in Drosophila. Loss of function mutations in *mesh1*, which encoded the ppGpp degrading enzyme led to longer sleep latency and less total sleep. These phenotypes could be rescued by wild type *mesh1*, but not by the enzymatically defective mutant Mesh1E66A, functionally implicating ppGpp. Ectopic expression of RelA, the *E. coli* synthetase for ppGpp, phenocopied *mesh1* knockout mutants, whereas overexpression of *mesh1* resulted in the opposite phenotypes, supporting that ppGpp is both necessary and sufficient in sleep regulation. *mesh1* is expressed in a specific population of neurons, and a chemoconnectomic screen followed by genetic intersection experiments implicate the pars intercerebralis (PI) as the site of ppGpp function. Our results have thus revealed that ppGpp is present in animals after long lag since its discovery in bacteria. Furthermore, we have demonstrated that ppGpp in a specific subset of neurons plays a physiological role in regulating sleep. We speculate that ppGpp may play function in mammals.

INTRODUCTION

It was 52 years ago when guanosine-5'-diphosphate, 3'-diphosphate (guanosine tetraphosphate, ppGpp) and guanosine-5'-triphosphate, 3'-diphosphate (guanosine pentaphosphate, pppGpp) were implicated in gene regulation in *Escherichia coli* (*E. coli*) (Cashel and Gallant, 1969). Collectively known as (p)ppGpp, they are key players in bacterial stringent response to amino acid starvation (Dalebroux and Swanson, 2012; Field, 2018; Gourse *et al*., 2018; Hauryliuk *et al*., 2015; Liu, Nbittner and Wang, 2015; Magnusson, Farewell and Nyström, 2005; Potrykus *et al*., 2008; Wang, Sanders and Grossman, 2007). The level of ppGpp is regulated by the RelA/SpoT Homolog (RSH) family (Haseltine and Block, 1973; Hogg *et al*., 2004). In bacteria, RelA is one of the RSHs (Haseltine and Block, 1973), which contains both a ppGpp synthetase domain (SYNTH) and an inactive ppGpp hydrolase domain (HD) (Hogg *et al*., 2004). When amino acids are depleted, uncharged tRNAs accumulate (Fangman and Neidhardt, 1964) and activate the ribosome-associated RelA (Yang and Ishiguro, 2001), which increases the production of ppGpp (Cochran and Byrne, 1974). Another typical RSH in bacteria is the ppGpp hydrolase SpoT (Laffler and Gallant, 1974), containing a weak SYNTH (Leung and Yamazaki, 1997) and an active HD (Murry and Bremer, 1996). Upon iron limitation (Vinella *et al*., 2005), carbon starvation (Lesley and Shapiro, 2008), or glucose phosphate stress (Kessler *et al*., 2017), ppGpp was also increased (Potrykus and Cashel, 2008).

ppGpp has also been detected in plants (Boniecka *et al*., 2017; Ito *et al*., 2012; Kaisai *et al*., 2004; Sugliani *et al*., 2016; Tozawa *et al*., 2007; van der Biezen *et al*.,

2000; Xiong *et al*., 2001). More than 30 members of the RSHs have been found in bacteria and plants (Atkinson *et al*., 2011; Field, 2018).

(p)ppGpp has not been detected in animals (Silverman and Atherly, 1979). Early report of ppGpp in the mouse turned out to be irreproducible (Irr, Kaulenas and Unsworth, 1974; Martini, Irr and Richter, 1977; Siverman and Atherly, 1977). Work in mammalian cell lines also failed to detect ppGpp before or after amino acid deprivation (Dabrowska *et al*., 2006a; Fan, Fisher and Edlin, 1973; Givens *et al*., 2004; Kim *et al*., 2009; Mamont *et al*., 1972; Rapaport and Bucher, 1976; Sato *et al*., 2015; Stanners and Thompson, 1974; Smulson, 1970; Takahashi *et al*., 2004; Thammana, Buerk and Gordon, 1976; Yamada *et al*., 2004). In Drosophila, Mesh1, a member of the RSH family containing only the hydrolase domain for ppGpp has been found (Sun *et al*., 2010), but ppGpp has not been detected.

Drosophila has served as a model for genetic studies of sleep for two decades (Hendricks *et al*., 2000, Shaw *et al*., 2000). Fly sleep is regulated by multiple genes functioning in several brain regions such as the fan-shape bodies (FSBs), the mushroom bodies, and the pars intercerebralis (PI) (e.g., Agosto *et al*., 2008; Andretic *et al*., 2005; Bushey *et al*., 2007; Cirelli *et al*., 2005; Crocker *et al*., 2010; Dai *et al*., 2019; Donlea *et al*., 2011, 2014; Guo *et al*., 2016; Hendericks *et al*., 2003; Koh *et al*., 2008; Kunst *et al*., 2014; Liu *et al*., 2014; Liu *et al*., 2016; Parisky *et al*., 2008; Qian *et al*., 2017; Shang *et al*., 2011; Sheeba *et al*., 2008; Sitaraman *et al*., 2015; Wu *et al*., 2010; Wu *et al*., 2014; Yuan *et al*., 2006; Yurgel *et al*., 2019).

We have carried out a genetic screen for genes involved in sleep regulation and

discovered that ppGpp is present in flies and regulates sleep. *mesh1* is expressed in a specific population of neurons, and the effects of RelA and Mesh1 overexpression could be detected when they were expressed in neurons, but not in non-neuronal cells. Further dissection narrowed down the functional significance of *mesh1* expressing neurons in the PI. Thus, after 52 years of its discovery, ppGpp has finally been found in animals and shown to play an important physiological role in specific neurons.

RESULTS

Discovery of ppGpp in Drosophila

We screened through 1765 P-element insertion lines of Drosophila for mutations affecting sleep latency (Eddison *et al*., 2012) (Figure 1A). An insertion in the *mesh1* gene (*mesh1*-ins) (Figure 1C) was found to have significantly longer sleep latency (Figure 1A and 1D) and less total sleep duration (Figure 1 B).

mesh1 encodes an RSH family member in animals (Sun *et al*., 2010). Mesh1 protein is predicted to have hydrolase activity, converting ppGpp to GDP (Figure 1E). We expressed the Drosophila Mesh1 protein in *E. coli* and purified it. In an in vitro hydrolysis assay with ppGpp, Mesh1 indeed degraded ppGpp (Figure S1A).

ppGpp has not been detected in animals (Hauryliuk *et al*., 2015; Sun *et al*., 2010). To measure endogenous ppGpp in Drosophila, extracts from more than 2000 flies were made. ppGpp was detected by ultra-performance liquid chromatography and mass spectrometry (UPLC-MS) in wild type (wt) flies (Figure 2A, 2B, 2D, 2E).

We generated a knockout (KO) line of *mesh1* (M1KO) using CRISPR-Cas9 to

replace most of its coding sequence following the start codon with 2A-attP (Figure 1C, S1B). More ppGpp was present in M1KO flies than the wt flies (Figure 2D and 2E), consistent with the fact that *mesh1* encoded only a hydrolase domain (Figure S1C). These results also supported that the ppGpp detected by us was regulated by the Drosophila *mesh1* gene.

The addition of Mesh1 protein to the extract from MIKO mutant flies also decreased the amount of ppGpp (Figure 2F).

Although ppGpp was detected and its level was regulated by the Drosophila *Mesh1* gene, which encoded an protein with ppGpp degrading activity, it remained possible that the detected ppGpp was synthesized from bacteria attached to flies. To test this possibility, we generated germ-free lines of wt and M1KO for analysis. We confirmed that the flies were indeed germ-free flies with both bacterial culture (Figure S1D) and 16S rDNA PCR (Figure S1E). ppGpp was detected in both fed and starved germ-free flies, and levels in M1KO were significantly higher in both conditions (Figure 2G, 2H).

Taken together, our results indicate that ppGpp exists in Drosophila.

Sleep Phenotypes of M1KO Mutant Flies

M1KO null *mesh1* mutants allowed us to investigate *mesh1* function in sleep (Figure 3A). In the paradigm of 12 hours light and 12 hours darkness (LD), M1KO flies showed decreased nighttime sleep (Figure 3B), decreased total sleep (Figure 3D) and increased sleep latency at night (Figure 3E), but no change in day time sleep level

(Figure 3C) or daytime sleep latency (Figure 3F). Sleep bout number and length either during the night or during the day were not significantly different between wt and M1KO flies (Figure S2A). Circadian rhythm was not significantly different between the wt and M1KO flies (Figure S2J, S2K, S2L and S2M). These results indicate that Mesh1 gene is mainly involved in regulating sleep latency.

We assessed awakening according to a procedure reported recently (Tabuchi *et al*., 2018). Awakening number at the beginning of nighttime sleep (dusk) (Figure 3G) and awakening number near the end of nighttime sleep (dawn) (Figure 3H) were significantly increased in M1KO mutants.

Under the constant darkness (DD) condition, the same phenotypes in sleep level (Figure S2B, S2D, S2E), latency (Figure S2F, S2G) and awakening (Figure S2H and S2I) were observed. Sleep level in presumptive day is decreased in W1KO flies under DD (Figure S2D), but not under LD condition (Figure 3C).

Requirement of the Enzymatic Activity in *mesh1* for Its Rescue of Sleep Phenotypes in M1KO Mutants

We generated another KO line of *mesh1* (M1KOGal4) by replacing its CDS after the start codon with an in-frame fusion of the 2A peptide and the yeast transcription factor Gal4 (Figure 4A and S1B). To examine whether *mesh1* gene functions in sleep through its regulation of ppGpp level, we compared the activities of the wt Mesh1 protein with that of the Mesh1 E66A mutant protein, both in vitro and in vivo.

Mesh1E66A expressed in bacteria could not hydrolyze ppGpp in vitro (Figure

S1A). Similar to that in M1KO mutants, the level of ppGpp in flies was also increased in M1KOGal4 (Figure S1G). ppGpp level was reduced to that of the wt flies when the wt *mesh1* gene was expressed in flies under the control of the M1KOGal4 driver (Figure S1G). By contrast, expression of *mesh1E66A* could not reduce the level of ppGpp in M1KOGal4 flies (Figure S1G). These results indicate that wt Mesh1 protein could, but Mesh1 E66A mutant protein could not, hydrolyze ppGpp either in vitro or in vivo.

M1KOGal4/M1KO flies were phenotypically similar to M1KO/M1KO in having longer sleep latencies (Figure 4B) and more awakening numbers (Figure 4D). Expression of UAS-*mesh1* driven by M1KOGal4 in the background of M1KOGal4/M1KO rescued all these phenotypes (Figure 4B to 4D). By contrast, UAS-*mesh1E66A* could not rescue the sleep phenotypes in M1KOGal4/M1KO flies (Figure 4B to 4D).

Taken together, the in vitro results from bacterially expressed Mesh1 and Mesh1E66A proteins and the in vivo results from genetic rescue experiments strongly support that ppGpp regulates sleep.

Pattern of *mesh1* Expression in Drosophila

To examine the expression pattern of the *mesh1* gene, we crossed M1KOGal4 with each of the following four UAS lines: UAS-mCD8-GFP for neuronal overviews (Lee and Luo, 1999), UAS-redStinger for nuclei (Barolo, Castro and Posakony, 2004), UAS-denmark for dendrites (Nikolai *et al*., 2010) and UAS-syt.eGFP for axon

terminals (Zhang, Rodesch and Broadie, 2002).

mesh1 was found in neurons in the brain and the ventral nerve cord (Figure 5A and 5E). In the brain, *mesh1* expressing neurons were detected in the PI and the suboesophageal ganglia (SOG) (Figure 5A and 5B). The *mesh1* expressing neurons in the PI and their axonal terminals in the SOG (Figure 5A, 5C and 5D) were reminiscent of the insulin-producing cells (IPC) in the PI which were shown previously to regulate sleep (Crocker *et al*., 2010). Immunostaining with an antibody for the *Drosophila* insulin like peptide 2 (Dilp2) confirmed expression of *mesh1* in IPC neurons positive in the PI (Figure S4C and S4E) (Li and Gong, 2015).

Evidence for ppGpp Functioning in Neurons

Because ppGpp regulate bacterial transcription through molecules such as the RNA polymerase ((Cashel and Gallant, 1969; Dalebroux and Swanson, 2012; Gourse *et al*., 2018; Hauryliuk *et al*., 2015; Magnusson, Farewell and Nyström, 2005; Potrykus *et al*., 2008; Wang, Sanders and Grossman, 2007), it is possible that ppGpp functions in many, even possibly all cells in animals. To test whether ppGpp functions in specific cells, we increased and decreased ppGpp levels in different populations of cells, by using ppGpp synthesizing and hydrolyzing enzymes.

The *E. coli RelA* gene encodes a synthetase for ppGpp (Laffler and Gallant, 1974). We confirmed that the RelA from *E. coli* used by us indeed increased ppGpp in vitro (Figure S1A). The biochemical activity of RelA protein is opposite to that of the Mesh1 protein, the effect of RelA overexpression in flies should be similar to *mesh1*

knockout mutation. In flies with UAS-RelA driven either by tub-Gal4 for expression in all cells (O'Donnell *et al*., 1994) or by elav-Gal4 for expression in neurons (Robinow and White, 1991), sleep latency (Figure 6A) and awakening number were increased (Figure 6B). By contrast, UAS-RelA driven by repo-Gal4 for expression in glial cells (Halter *et al*., 1995) did not affect sleep (Figure 6A and 6B). These results indicate that ppGpp regulation of sleep does not involve glial cells, but specifically neurons.

Furthermore, when M1KOGal4 was used to drive UAS-RelA expression, both sleep latency (Figure 6A) and awakening numbers (Figure 6B) were significantly increased, indicating that ppGpp level in *mesh1* positive neurons is sufficient to regulate sleep.

To decrease ppGpp level in fly cells, we used UAS-*mesh1*. UAS-*mesh1* overexpression driven by tub-Gal4 in all cells or by elav-Gal4 in neurons significantly decreased sleep latency (Figure 7A) and awakening numbers (Figure 7B). By contrast, UAS-*mesh1* overexpression driven by repo-Gal4 in glial cells did not affect sleep latency or awakening numbers (Figure 7A and 7B). When UAS-*mesh1* was driven by Mesh1 Gal4, sleep latency and awakening number were decreased (Figure 7A and 7B).

Taken together, data from increasing or decreasing the ppGpp level by RelA and Mesh1 indicate that ppGpp functions in neurons but not in glia to regulate sleep.

Dissection of PI Neurons Involved in ppGpp Regulation of Sleep

Our results have shown that neurons, specifically, *mesh1* expressing neurons, are required for ppGpp regulation of sleep (Figure 4B, 4C, 4D, 6A, 6B, 7A and 7B). We have generated a Gal4 library for the chemoconnectome (CCT), which include all the known neurotransmitters, modulators, neuropeptides and their receptors (Deng *et al*., 2019). We carried out a CCT screen by crossing each Gal4 line with UAS-RelA. RelA expression driven by Gal4 lines for Trh, Capa-R, CCHa2-R, LkR, OA2 and CG13229 affected sleep (Figure S3A). It was noted that all of these lines drove expression in the PI (Figure S3 B to G). This suggests functional significance of *mesh1* expression in the PI (Figure 5).

To further dissect the PI neurons for functional involvement in ppGpp regulation of sleep, we tested five Gal4 lines known to drive expression in PI neurons: a line for PI (c767, Cavanaugh *et al*., 2014; Donlea *et al*., 2009), three lines for neuropeptides Dh44 (Cannel *et al*., 2016; Chen and Dahanukar, 2018), Dilp2 (Crocker *et al*., 2010; Semaniuk *et al*., 2018; Yurgel *et al*., 2019) and SIFa (Martelli *et al*., 2017; Park *et al*., 2014), and one line for receptor R19G10 (an RYamide receptor) (Collins *et al*., 2011; Ohno *et al*., 2017). We crossed each of these PI drivers to a line of knockin flies with in-frame fusion of the flippase gene to the C terminus of the *mesh1* gene (M1KIflp) (Figure S4A), which was recombined with UAS-FRT-stop-FRT-mCD8-GFP as a reporter. Expression of *mesh1* gene in these specific PI neurons were confirmed (Figure S4B, S4C and S4D).

Each of these PI drivers was crossed with UAS-RelA to increase ppGpp level in specific neurons. Sleep latency (Figure 6C) and awakening (Figure 6D) were

234 increased by RelA expression (Figure 6C and 6D) in neurons expressing Dilp2, SIFa,
235 R19G10 or c767. However, RelA expression in Dh44 neurons could affect sleep
236 (Figure 6C and 6D)

237 Each of these PI drivers was crossed with UAS-Mesh1 to decrease ppGpp level
238 in specific neurons. Overexpression of Mesh1 in Dilp2 neurons decreased sleep
239 latency and awakening (Figure 7D, 7E and 7F). Sleep latency and awakening were
240 decreased by Mesh1 expression in neurons positive for Dilp2, SIFa, R19G10 or c767
241 (Figure 7D and 7E). However, Mesh1 expression in Dh44 neurons could affect sleep
242 (Figure 7D and 7E).

243 Taken together, experiments with RelA and Mesh1 expression have provided
244 consistent results indicating that specific subsets of neurons in the PI are involved in
245 ppGpp regulation of sleep.

246

247 **Role of ppGpp in Starvation Induced Sleep Loss**

248 We investigated whether ppGpp played a role in starvation induced sleep loss (SISL).
249 Similar to humans (MacFadyen, Oswald and Lewis, 1973), flies also show SISL
250 (Keene *et al*., 2010). Baseline sleep in fed flies was recorded before flies were starved
251 for 24 hours (Yurgel *et al*., 2019). Sleep during starvation was compared to that before
252 starvation (Figure 8A).

253 When *mesh1* gene was deleted in M1KO, nighttime SISL in M1KO flies was
254 significantly more than that in wt flies, whereas daytime SISL were similar between
255 the wt and M1KO mutant flies (Figure 8A and 8B). Although nighttime sleep latency

during starvation night was still higher in M1KO (Figure S6A and S6B), there was no latency change after starvation during either night time or day time (Figure S6C and S6D). The M1KOGal4 knockin mutants were similar to M1KO flies in having exacerbated SISL (Figure 8C and S5). UAS-*mesh1* but not UAS-*mesh1E66A* could rescue the phenotype of SISL in mesh1 knockout flies, indicating that the ppGpp hydrolyzing activity is required for Mesh1 involvement in SISL. Expression of the bacterial ppGpp synthesizing enzyme RelA caused a decrease in SISL (Figure 8D), opposite to the SISL enhancing effect of Mesh1 (Figure 9A), indicating that ppGpp level, rather than any other unexpected activities of RelA or Mesh1 were involved.

SISL was increased by general or neuronal expression of RelA, but not by glial expression of RelA (Figure 8D, 9A and 9C). SISL was decreased by general or neuronal overexpression of Mesh1, but not by glial overexpression of Mesh1 (Figure 9A and 9C).

SISL was enhanced by RelA expression driven by Gal4 lines for c767, Dilp2, SIFamide or R19G10 (Figure 8E). SISL was reduced by Mesh1 overexpression driven by Gal4 lines for c767, Dilp2, SIFamide or R19G10 (Figure 9B, 9D). By contrast, Dh44 expressing neurons were not involved in ppGpp regulation of SISL because neither RelA expression nor Mesh1 overexpression in Dh44 neurons affected SISL (Figure 8E, 9B and 9D).

Thus, the same neurons required for ppGpp regulation of sleep latency and awakening are also involved in its regulation of SISL.

DISCUSSION

We have discovered a new molecule in animals and provided evidence that it plays a physiological role. These results came from integrated genetic and chemical approaches. We have carried out a genetic screen of P element insertion lines which led to the discovery of a new mutation in the Drosophila ppGpp hydrolase Mesh1. Our chemical analyses indicate that ppGpp is present in Drosophila, not a contaminant of bacteria: germ free flies still had ppGpp and the content of ppGpp is regulated both by an enzyme encoded by a Drosophila gene and by starvation of flies. Our chemoconnectomic screen suggests involvement of PI neurons in ppGpp function. Further genetic intersection experiments confirm that ppGpp in specific PI neurons regulate sleep. Our findings indicate that ppGpp is not just a molecule present in prokaryotes and plants, but also exists and functions in animals. It regulates sleep, including sleep latency and SISL.

Evidence for ppGpp Presence in Drosophila

We have shown that ppGpp is present in Drosophila and that it is hydrolyzed by Mesh1 which are expressed in specific neurons in flies. Moreover, ppGpp is detected in germ-free flies, indicating that ppGpp is synthesized in Drosophila (Figure 2G, 2H), not a contaminant of bacteria.

RSHs with the synthetase domain exist in both bacteria (Cochran and Byrne, 1974) and plants (van der Biezen *et al*., 2000), but not in animals (Atkinson *et al*., 2011; Sun *et al*., 2010). Our results suggest that the presence of a ppGpp synthetase in

300 animals which does not contain an RSH like domain.

301 Plant RSHs are thought to result from lateral gene transfer events from bacteria
302 (Ito *et al*., 2017; Field, 2018). Bioinformatic analyses and biochemical assays indicate
303 that ppGpp synthetase homologs are distributed widely in plants including:
304 dicotyledon A. thalaniana (van der Biezen *et al*., 2000), monocotyledon O. sativa
305 (Xiong *et al*., 2001), green algae C. reinhardtii (Kasai *et al*., 2002), S. japonica
306 (Yamada *et al*., 2004), N. Tabacum (Givens *et al*., 2004), pea plants (Takahashi *et al*.,
307 2004), P. nil (Dabrowska *et al*., 2006a), C. annnum (Kim *et al*., 2009), and moss P.
308 patens (Sato *et al*., 2015). Presence of the N-terminal chloroplast transit peptide (cTP),
309 causes most plant RSHs to be located in the chloroplasts (Boniecka *et al*., 2017; Chen
310 *et al*., 2014; Mizusawa *et al*., 2008; Takahashi *et al*., 2004; Sugliani *et al*., 2016; Sato
311 *et al*., 2009; Takahashi *et al*., 2004). It is unclear whether a ppGpp synthetase exists in
312 Drosophila mitochondria.

313

314 **Evidence for ppGpp Function in Drosophila**

315 We obtain evidence for ppGpp function from four lines of experiments. First, three
316 mutations in mesh1 caused sleep phenotypes in Drosophila. The first mutation is a
317 P-element insertion (Eddison *et al*., 2012), whose phenotype (Figure 1A and 1B) and
318 molecular nature we have characterized as *mesh1-ins* (Figure 1C). The second
319 mutation is a knockout generated by us as M1KO (Figure 4A top panel). The third
320 mutation is a knockin generated by us as M1KOGal4 (Figure 4A bottom panel). All
321 three lines have the same phenotypes (Figure 1, 3 and 4).

Second, we have shown that the hydrolyzing activity of Mesh1 is required to rescue the *mesh1* knockout mutant phenotype: if a point mutation was introduced to amino acid residue 66 by converting it from E to A, then it was enzymatically inactive in vitro (Figure S1C and S1D) and unable to rescue the sleep phenotype in vivo (Figure 4B, 4C, 4D and 8C).

Third, expression of RelA, a bacterial ppGpp synthetase, in Drosophila phenocopied *mesh1* knockout mutants (Figure 6, 8D and 8E).

Fourth, the phenotypes of Mesh1 overexpression are opposite to those of RelA expression (Figure 7 and 9).

Function of ppGpp in Neurons

Does ppGpp function in all cells or only in some cells? Results obtained here support that ppGpp functions in specific neurons in the PI to regulate sleep.

Mesh1 gene has been found to be expressed in specific neurons (Figure 5). Because Mesh1 is a ppGpp hydrolase, its expression can show the location where ppGpp is hydrolyzed, but not necessarily where it is synthesized or where it functions. When we used Gal4 lines from CCT to drive the expression of RelA, sleep phenotypes were observed in 6 lines which were all expressed in the PI (Figure 7). When Gal4 lines for PI neurons were used to drive RelA or Mesh1 expression, several of them could indeed cause sleep phenotypes (Figure 6, 7, 8 and 9). Expression of RelA or Mesh1 in glial cells did not affect sleep (Figure 6A, 6B, 7A and 7B).

Because it is difficult to imagine that both synthetase and hydrolase could cause

the same multiple phenotypes in the same neurons if these neurons are not where ppGpp functions, our results are most consistent with the idea that ppGpp functions in these PI neurons.

Molecular Targets of ppGpp

In bacteria, the best-known direct target of ppGpp is RNA polymerase (RNAP) (e.g., Artsimovitch *et al*., 2004; Barker *et al*., 2001; Kajitani and Ishihama, 1984; Kingston *et al*., 1981; Lindahl and Nomura, 1976). ppGpp interaction with the RNA polymerase leads to blockage of transcription initiation (Artsimovitch *et al*., 2004) and elongation (Kingston *et al*., 1981). There are also other targets for ppGpp (e.g., Paul *et al*., 2005); Gourse *et al*., 2018; Maciag *et al*., 2010; Nomura *et al*., 2014; Sherlock *et al*., 2018; Corrigan *et al*., 2016; Pao and Dyess, 1981; Dalebroux and Swanson, 2012; Zhang *et al*., 2019). A recent study utilizing a ppGpp-coupled bait uncovered new ppGpp target proteins in bacteria, including a large group of GTPase and metabolism-related enzymes (Wang *et al*., 2019). Future studies are required to identify the molecule(s) directly mediating the sleep regulating function of ppGpp in Drosophila.

SUPPLEMENTAL INFORMATION

Supplemental information includes 6 Figure.

ACKNOWLEDGEMENTS

We are grateful to Dr. U. Heberlein for sharing P-element insertion mutant library, Drs. J. Ni and G. Gao for providing us with CRISPR/Cas9 plasmids and flies, to Dr. Z.-F. Gong for sharing antibodies, to the Beijing Commission of Science and Technology and the National Natural Science Foundation of China (Project 31421003 to Y. R.) for grant support.

AUTHOR CONTRIBUTIONS

Y.R supervised and initiated the project. W. Y. performed the majority of experiments and data analysis. X. H. W. carried our experiments of UPLC-MS. W. Y., E. Z. and H. D. X. carried out experiments of sleep screen on P-element insertion mutants. W. Y. implemented the fly tracing program, and E. Z. developed software for sleep analyses. W. Y. and Y. R. wrote the manuscript.

DECLARATION OF INTERESTS

The authors declare no competing interests.

REFERENCES

Akerboom, J., Chen, T.W., Wardill, T.J., Tian, L., Marvin, J.S., Mutlu, S., Calderon, N.C., Esposti, F., Borghuis, B.G., Sun, X.R., et al. (2012). Optimization of a GCaMP calcium indicator for neural activity imaging. J Neurosci 32, 13819-13840.

Andretic, R., van Swinderen, B., and Greenspan, R.J. (2005). Dopaminergic modulation of arousal in Drosophila. Curr Biol 15, 1165-1175.

Artsimovitch, I., Patlan, V., Sekine, S., Vassylyeva, M.N., Hosaka, T., Ochi, K., Yokoyama, S., and Vassylyev, D.G. (2004). Structural basis for transcription regulation by alarmone ppGpp. Cell 117, 299-310.

Atkinson, G.C., Tenson, T., and Hauryliuk, V. (2011). The RelA/SpoT homolog (RSH) superfamily: distribution and functional evolution of ppGpp synthetases and hydrolases across the tree of life. PLoS One 6, e23479.

Beilstein, K., Wittmann, A., Grez, M., and Suess, B. (2015). Conditional control of mammalian gene expression by tetracycline-dependent hammerhead ribozymes. ACS Synth Biol 4, 526-534.

Boniecka, J., Prusinska, J., Dabrowska, G.B., and Goc, A. (2017). Within and beyond the stringent response-RSH and (p)ppGpp in plants. Planta 246, 817-842.

Braselmann, E., Wierzba, A.J., Polaski, J.T., Chrominski, M., Holmes, Z.E., Hung, S.T., Batan, D., Wheeler, J.R., Parker, R., Jimenez, R., et al. (2018). A multicolor riboswitch-based platform for imaging of RNA in live mammalian cells. Nat Chem Biol 14, 964-971.

Bushey, D., Huber, R., Tononi, G., and Cirelli, C. (2007). Drosophila Hyperkinetic mutants have reduced sleep and impaired memory. J Neurosci 27, 5384-5393.

Cannell, E., Dornan, A.J., Halberg, K.A., Terhzaz, S., Dow, J.A.T., and Davies, S.A. (2016). The corticotropin-releasing factor-like diuretic hormone 44 (DH44) and kinin neuropeptides modulate desiccation and starvation tolerance in Drosophila melanogaster. Peptides 80, 96-107.

Carter, M.E., Han, S., and Palmiter, R.D. (2015). Parabrachial calcitonin gene-related peptide neurons mediate conditioned taste aversion. J Neurosci 35, 4582-4586.

Cashel, M., and Gallant, J. (1969). Two compounds implicated in the function of the RC gene of Escherichia coli. Nature 221, 838-841.

Cavanaugh, D.J., Geratowski, J.D., Wooltorton, J.R., Spaethling, J.M., Hector, C.E., Zheng, X., Johnson, E.C., Eberwine, J.H., and Sehgal, A. (2014). Identification of a circadian output circuit for rest:activity rhythms in Drosophila. Cell 157, 689-701.

Cavey, M., Collins, B., Bertet, C., and Blau, J. (2016). Circadian rhythms in neuronal activity propagate through output circuits. Nat Neurosci 19, 587-595.

Chen, Y.D., and Dahanukar, A. (2018). DH44 neurons: gut-brain amino acid sensors. Cell Res 28, 1048-1049.

Cochran, J.W., and Byrne, R.W. (1974). Isolation and properties of a ribosome-bound factor required for ppGpp and ppGpp synthesis in Escherichia coli. J Biol Chem 249, 353-360.

Coll, A.P., Farooqi, I.S., and O'Rahilly, S. (2007). The hormonal control of food intake. Cell 129, 251-262.

Collin, C., Hauser, F., Krogh-Meyer, P., Hansen, K.K., Gonzalez de Valdivia, E.,

427 Williamson, M., and Grimmelikhuijzen, C.J. (2011). Identification of the Drosophila
428 and Tribolium receptors for the recently discovered insect RYamide neuropeptides.
429 Biochem Biophys Res Commun 412, 578-583.
430 Corrigan, R.M., Bellows, L.E., Wood, A., and Grundling, A. (2016). ppGpp
431 negatively impacts ribosome assembly affecting growth and antimicrobial tolerance in
432 Gram-positive bacteria. Proc Natl Acad Sci U S A 113, E1710-1719.
433 Crocker, A., and Sehgal, A. (2008). Octopamine regulates sleep in drosophila through
434 protein kinase A-dependent mechanisms. J Neurosci 28, 9377-9385.
435 Crocker, A., Shahidullah, M., Levitan, I.B., and Sehgal, A. (2010). Identification of a
436 neural circuit that underlies the effects of octopamine on sleep:wake behavior. Neuron
437 65, 670-681.
438 Dalebroux, Z.D., and Swanson, M.S. (2012). ppGpp: magic beyond RNA polymerase.
439 Nat Rev Microbiol 10, 203-212.
440 Dennis, P.P., and Nomura, M. (1975). Regulation of the expression of ribosomal
441 protein genes in Escherichia coli. J Mol Biol 97, 61-76.
442 Donlea, J.M. (2017). Neuronal and molecular mechanisms of sleep homeostasis. Curr
443 Opin Insect Sci 24, 51-57.
444 Donlea, J.M., Ramanan, N., and Shaw, P.J. (2009). Use-dependent plasticity in clock
445 neurons regulates sleep need in Drosophila. Science 324, 105-108.
446 Donlea, J.M., Thimgan, M.S., Suzuki, Y., Gottschalk, L., and Shaw, P.J. (2011).
447 Inducing sleep by remote control facilitates memory consolidation in Drosophila.
448 Science 332, 1571-1576.
449 Fangman, W.L., and Neidhardt, F.C. (1964). Protein and Ribonucleic Acid Synthesis
450 in a Mutant of Escherichia Coli with an Altered Aminoacyl Ribonucleic Acid
451 Synthetase. J Biol Chem 239, 1844-1847.
452 Field, B. (2018). Green magic: regulation of the chloroplast stress response by
453 (p)ppGpp in plants and algae. J Exp Bot 69, 2797-2807.
454 Givens, R.M., Lin, M.H., Taylor, D.J., Mechold, U., Berry, J.O., and Hernandez, V.J.
455 (2004). Inducible expression, enzymatic activity, and origin of higher plant
456 homologues of bacterial RelA/SpoT stress proteins in Nicotiana tabacum. J Biol
457 Chem 279, 7495-7504.
458 Gourse, R.L., Chen, A.Y., Gopalkrishnan, S., Sanchez-Vazquez, P., Myers, A., and
459 Ross, W. (2018). Transcriptional Responses to ppGpp and DksA. Annu Rev Microbiol
460 72, 163-184.
461 Halter, D.A., Urban, J., Rickert, C., Ner, S.S., Ito, K., Travers, A.A., and Technau,
462 G.M. (1995). The homeobox gene repo is required for the differentiation and
463 maintenance of glia function in the embryonic nervous system of Drosophila
464 melanogaster. Development 121, 317-332.
465 Harbaugh, S.V., Goodson, M.S., Dillon, K., Zabarnick, S., and Kelley-Loughnane, N.
466 (2017). Riboswitch-Based Reversible Dual Color Sensor. ACS Synth Biol 6, 766-781.
467 Haseltine, W.A., and Block, R. (1973). Synthesis of guanosine tetra- and
468 pentaphosphate requires the presence of a codon-specific, uncharged transfer
469 ribonucleic acid in the acceptor site of ribosomes. Proc Natl Acad Sci U S A 70,
470 1564-1568.

Hauryliuk, V., Atkinson, G.C., Murakami, K.S., Tenson, T., and Gerdes, K. (2015). Recent functional insights into the role of (p)ppGpp in bacterial physiology. Nat Rev Microbiol 13, 298-309.

Hendricks, J.C., Finn, S.M., Panckeri, K.A., Chavkin, J., Williams, J.A., Sehgal, A., and Pack, A.I. (2000). Rest in Drosophila is a sleep-like state. Neuron 25, 129-138.

Hendricks, J.C., Lu, S., Kume, K., Yin, J.C., Yang, Z., and Sehgal, A. (2003). Gender dimorphism in the role of cycle (BMAL1) in rest, rest regulation, and longevity in Drosophila melanogaster. J Biol Rhythms 18, 12-25.

Hesketh, A., Vergnano, M., Wan, C., and Oliver, S.G. (2017). Bacterial Signaling Nucleotides Inhibit Yeast Cell Growth by Impacting Mitochondrial and Other Specifically Eukaryotic Functions. MBio 8.

Hogg, T., Mechold, U., Malke, H., Cashel, M., and Hilgenfeld, R. (2004). Conformational antagonism between opposing active sites in a bifunctional RelA/SpoT homolog modulates (p)ppGpp metabolism during the stringent response [corrected]. Cell 117, 57-68.

Hummel, T., and Klambt, C. (2008). P-element mutagenesis. Methods Mol Biol 420, 97-117.

Hwang, E., Song, J., and Zhang, J. (2019). Integration of Nanomaterials and Bioluminescence Resonance Energy Transfer Techniques for Sensing Biomolecules. Biosensors (Basel) 9.

Ida, T., Takahashi, T., Tominaga, H., Sato, T., Kume, K., Ozaki, M., Hiraguchi, T., Maeda, T., Shiotani, H., Terajima, S., et al. (2011). Identification of the novel bioactive peptides dRYamide-1 and dRYamide-2, ligands for a neuropeptide Y-like receptor in Drosophila. Biochem Biophys Res Commun 410, 872-877.

Jenett, A., Rubin, G.M., Ngo, T.T., Shepherd, D., Murphy, C., Dionne, H., Pfeiffer, B.D., Cavallaro, A., Hall, D., Jeter, J., et al. (2012). A GAL4-driver line resource for Drosophila neurobiology. Cell Rep 2, 991-1001.

Kasai, K., Kanno, T., Endo, Y., Wakasa, K., and Tozawa, Y. (2004). Guanosine tetra- and pentaphosphate synthase activity in chloroplasts of a higher plant: association with 70S ribosomes and inhibition by tetracycline. Nucleic Acids Res 32, 5732-5741.

Kasai, K., Usami, S., Yamada, T., Endo, Y., Ochi, K., and Tozawa, Y. (2002). A RelA-SpoT homolog (Cr-RSH) identified in Chlamydomonas reinhardtii generates stringent factor in vivo and localizes to chloroplasts in vitro. Nucleic Acids Res 30, 4985-4992.

Kessler, J.R., Cobe, B.L., and Richards, G.R. (2017). Stringent Response Regulators Contribute to Recovery from Glucose Phosphate Stress in Escherichia coli. Appl Environ Microbiol 83.

Kietz, C., Pollari, V., and Meinander, A. (2018). Generating Germ-Free Drosophila to Study Gut-Microbe Interactions: Protocol to Rear Drosophila Under Axenic Conditions. Curr Protoc Toxicol 77, e52.

King, A.N., Barber, A.F., Smith, A.E., Dreyer, A.P., Sitaraman, D., Nitabach, M.N., Cavanaugh, D.J., and Sehgal, A. (2017). A Peptidergic Circuit Links the Circadian Clock to Locomotor Activity. Curr Biol 27, 1915-1927 e1915.

Kingston, R.E., Nierman, W.C., and Chamberlin, M.J. (1981). A direct effect of

515 guanosine tetraphosphate on pausing of Escherichia coli RNA polymerase during
516 RNA chain elongation. J Biol Chem 256, 2787-2797.
517 Koh, K., Joiner, W.J., Wu, M.N., Yue, Z., Smith, C.J., and Sehgal, A. (2008).
518 Identification of SLEEPLESS, a sleep-promoting factor. Science 321, 372-376.
519 Kunst, M., Hughes, M.E., Raccuglia, D., Felix, M., Li, M., Barnett, G., Duah, J., and
520 Nitabach, M.N. (2014). Calcitonin gene-related peptide neurons mediate
521 sleep-specific circadian output in Drosophila. Curr Biol 24, 2652-2664.
522 Laffler, T., and Gallant, J.A. (1974). Stringent control of protein synthesis in E. coli.
523 Cell 3, 47-49.
524 Lesley, J.A., and Shapiro, L. (2008). SpoT regulates DnaA stability and initiation of
525 DNA replication in carbon-starved Caulobacter crescentus. J Bacteriol 190,
526 6867-6880.
527 Leung, K.L., and Yamazaki, H. (1977). Synthesis of pppGpp by ribosomes from an
528 Escherichia coli spoT mutant and the metabolic relationship between pppGpp and
529 ppGpp. Can J Biochem 55, 1207-1212.
530 Li, Q., and Gong, Z. (2015). Cold-sensing regulates Drosophila growth through
531 insulin-producing cells. Nat Commun 6, 10083.
532 Liu, K., Bittner, A.N., and Wang, J.D. (2015). Diversity in (p)ppGpp metabolism and
533 effectors. Curr Opin Microbiol 24, 72-79.
534 Liu, S., Liu, Q., Tabuchi, M., and Wu, M.N. (2016). Sleep Drive Is Encoded by
535 Neural Plastic Changes in a Dedicated Circuit. Cell 165, 1347-1360.
536 Maciag, M., Kochanowska, M., Lyzen, R., Wegrzyn, G., and Szalewska-Palasz, A.
537 (2010). ppGpp inhibits the activity of Escherichia coli DnaG primase. Plasmid 63,
538 61-67.
539 Martelli, C., Pech, U., Kobbenbring, S., Pauls, D., Bahl, B., Sommer, M.V., Pooryasin,
540 A., Barth, J., Arias, C.W.P., Vassiliou, C., et al. (2017). SIFamide Translates Hunger
541 Signals into Appetitive and Feeding Behavior in Drosophila. Cell Rep 20, 464-478.
542 Murray, K.D., and Bremer, H. (1996). Control of spoT-dependent ppGpp synthesis
543 and degradation in Escherichia coli. J Mol Biol 259, 41-57.
544 Nomura, Y., Kumar, D., and Yokobayashi, Y. (2012). Synthetic mammalian
545 riboswitches based on guanine aptazyme. Chem Commun (Camb) 48, 7215-7217.
546 O'Donnell, K.H., Chen, C.T., and Wensink, P.C. (1994). Insulating DNA directs
547 ubiquitous transcription of the Drosophila melanogaster alpha 1-tubulin gene. Mol
548 Cell Biol 14, 6398-6408.
549 Obadia, B., Guvener, Z.T., Zhang, V., Ceja-Navarro, J.A., Brodie, E.L., Ja, W.W., and
550 Ludington, W.B. (2017). Probabilistic Invasion Underlies Natural Gut Microbiome
551 Stability. Curr Biol 27, 1999-2006 e1998.
552 Pao, C.C., and Dyess, B.T. (1981). Effect of unusual guanosine nucleotides on the
553 activities of some Escherichia coli cellular enzymes. Biochim Biophys Acta 677,
554 358-362.
555 Parisky, K.M., Agosto, J., Pulver, S.R., Shang, Y., Kuklin, E., Hodge, J.J., Kang, K.,
556 Liu, X., Garrity, P.A., Rosbash, M., et al. (2008). PDF cells are a GABA-responsive
557 wake-promoting component of the Drosophila sleep circuit. Neuron 60, 672-682.
558 Park, S., Sonn, J.Y., Oh, Y., Lim, C., and Choe, J. (2014). SIFamide and SIFamide

559 receptor defines a novel neuropeptide signaling to promote sleep in Drosophila. Mol
560 Cells 37, 295-301.
561 Paul, B.J., Berkmen, M.B., and Gourse, R.L. (2005). DksA potentiates direct
562 activation of amino acid promoters by ppGpp. Proc Natl Acad Sci U S A 102,
563 7823-7828.
564 Peselis, A., and Serganov, A. (2018). ykkC riboswitches employ an add-on helix to
565 adjust specificity for polyanionic ligands. Nat Chem Biol 14, 887-894.
566 Potrykus, K., and Cashel, M. (2008). (p)ppGpp: still magical? Annu Rev Microbiol 62,
567 35-51.
568 Qian, Y., Cao, Y., Deng, B., Yang, G., Li, J., Xu, R., Zhang, D., Huang, J., and Rao, Y.
569 (2017). Sleep homeostasis regulated by 5HT2b receptor in a small subset of neurons
570 in the dorsal fan-shaped body of drosophila. Elife 6.
571 Ren, X., Sun, J., Housden, B.E., Hu, Y., Roesel, C., Lin, S., Liu, L.P., Yang, Z., Mao,
572 D., Sun, L., et al. (2013). Optimized gene editing technology for Drosophila
573 melanogaster using germ line-specific Cas9. Proc Natl Acad Sci U S A 110,
574 19012-19017.
575 Robinow, S., and White, K. (1991). Characterization and spatial distribution of the
576 ELAV protein during Drosophila melanogaster development. J Neurobiol 22,
577 443-461.
578 Ross, W., Vrentas, C.E., Sanchez-Vazquez, P., Gaal, T., and Gourse, R.L. (2013). The
579 magic spot: a ppGpp binding site on E. coli RNA polymerase responsible for
580 regulation of transcription initiation. Mol Cell 50, 420-429.
581 Sato, M., Takahashi, K., Ochiai, Y., Hosaka, T., Ochi, K., and Nabeta, K. (2009).
582 Bacterial alarmone, guanosine 5'-diphosphate 3'-diphosphate (ppGpp), predominantly
583 binds the beta' subunit of plastid-encoded plastid RNA polymerase in chloroplasts.
584 Chembiochem 10, 1227-1233.
585 Schretter, C.E., Vielmetter, J., Bartos, I., Marka, Z., Marka, S., Argade, S., and
586 Mazmanian, S.K. (2018). A gut microbial factor modulates locomotor behaviour in
587 Drosophila. Nature 563, 402-406.
588 Selkrig, J., Mohammad, F., Ng, S.H., Chua, J.Y., Tumkaya, T., Ho, J., Chiang, Y.N.,
589 Rieger, D., Pettersson, S., Helfrich-Forster, C., et al. (2018). The Drosophila
590 microbiome has a limited influence on sleep, activity, and courtship behaviors. Sci
591 Rep 8, 10646.
592 Semaniuk, U.V., Gospodaryov, D.V., Feden'ko, K.M., Yurkevych, I.S., Vaiserman,
593 A.M., Storey, K.B., Simpson, S.J., and Lushchak, O. (2018). Insulin-Like Peptides
594 Regulate Feeding Preference and Metabolism in Drosophila. Front Physiol 9, 1083.
595 Shang, Y., Haynes, P., Pirez, N., Harrington, K.I., Guo, F., Pollack, J., Hong, P.,
596 Griffith, L.C., and Rosbash, M. (2011). Imaging analysis of clock neurons reveals
597 light buffers the wake-promoting effect of dopamine. Nat Neurosci 14, 889-895.
598 Shaw, J., and Brody, S. (2000). Circadian rhythms in Neurospora: a new measurement,
599 the reset zone. J Biol Rhythms 15, 225-240.
600 Sheeba, V., Fogle, K.J., Kaneko, M., Rashid, S., Chou, Y.T., Sharma, V.K., and
601 Holmes, T.C. (2008). Large ventral lateral neurons modulate arousal and sleep in
602 Drosophila. Curr Biol 18, 1537-1545.

603 Sherlock, M.E., Sudarsan, N., and Breaker, R.R. (2018). Riboswitches for the
604 alarmone ppGpp expand the collection of RNA-based signaling systems. Proc Natl
605 Acad Sci U S A 115, 6052-6057.
606 Shin, S.C., Kim, S.H., You, H., Kim, B., Kim, A.C., Lee, K.A., Yoon, J.H., Ryu, J.H.,
607 and Lee, W.J. (2011). Drosophila microbiome modulates host developmental and
608 metabolic homeostasis via insulin signaling. Science 334, 670-674.
609 Sitaraman, D., Aso, Y., Jin, X., Chen, N., Felix, M., Rubin, G.M., and Nitabach, M.N.
610 (2015). Propagation of Homeostatic Sleep Signals by Segregated Synaptic
611 Microcircuits of the Drosophila Mushroom Body. Curr Biol 25, 2915-2927.
612 Schmid, B., Helfrich-Forster, C., and Yoshii, T. (2011). A new ImageJ plug-in
613 "ActogramJ" for chronobiological analyses. J Biol Rhythms 26, 464-467.
614 Sitaraman, D., Zars, M., Laferriere, H., Chen, Y.C., Sable-Smith, A., Kitamoto, T.,
615 Rottinghaus, G.E., and Zars, T. (2008). Serotonin is necessary for place memory in
616 Drosophila. Proc Natl Acad Sci U S A 105, 5579-5584.
617 Sugliani, M., Abdelkefi, H., Ke, H., Bouveret, E., Robaglia, C., Caffarri, S., and Field,
618 B. (2016). An Ancient Bacterial Signaling Pathway Regulates Chloroplast Function to
619 Influence Growth and Development in Arabidopsis. Plant Cell 28, 661-679.
620 Sun, D., Lee, G., Lee, J.H., Kim, H.Y., Rhee, H.W., Park, S.Y., Kim, K.J., Kim, Y.,
621 Kim, B.Y., Hong, J.I., et al. (2010). A metazoan ortholog of SpoT hydrolyzes ppGpp
622 and functions in starvation responses. Nat Struct Mol Biol 17, 1188-1194.
623 Sun, F., Zeng, J., Jing, M., Zhou, J., Feng, J., Owen, S.F., Luo, Y., Li, F., Wang, H.,
624 Yamaguchi, T., et al. (2018). A Genetically Encoded Fluorescent Sensor Enables
625 Rapid and Specific Detection of Dopamine in Flies, Fish, and Mice. Cell 174,
626 481-496 e419.
627 Tabuchi, M., Monaco, J.D., Duan, G., Bell, B., Liu, S., Liu, Q., Zhang, K., and Wu,
628 M.N. (2018). Clock-Generated Temporal Codes Determine Synaptic Plasticity to
629 Control Sleep. Cell 175, 1213-1227 e1218.
630 Takahashi, K., Kasai, K., and Ochi, K. (2004). Identification of the bacterial alarmone
631 guanosine 5'-diphosphate 3'-diphosphate (ppGpp) in plants. Proc Natl Acad Sci U S A
632 101, 4320-4324.
633 Tozawa, Y., and Nomura, Y. (2011). Signalling by the global regulatory molecule
634 ppGpp in bacteria and chloroplasts of land plants. Plant Biol (Stuttg) 13, 699-709.
635 Tozawa, Y., Nozawa, A., Kanno, T., Narisawa, T., Masuda, S., Kasai, K., and
636 Nanamiya, H. (2007). Calcium-activated (p)ppGpp synthetase in chloroplasts of land
637 plants. J Biol Chem 282, 35536-35545.
638 Trinder, M., Daisley, B.A., Dube, J.S., and Reid, G. (2017). Drosophila melanogaster
639 as a High-Throughput Model for Host-Microbiota Interactions. Front Microbiol 8,
640 751.
641 van der Biezen, E.A., Sun, J., Coleman, M.J., Bibb, M.J., and Jones, J.D. (2000).
642 Arabidopsis RelA/SpoT homologs implicate (p)ppGpp in plant signaling. Proc Natl
643 Acad Sci U S A 97, 3747-3752.
644 Venken, K.J., Schulze, K.L., Haelterman, N.A., Pan, H., He, Y., Evans-Holm, M.,
645 Carlson, J.W., Levis, R.W., Spradling, A.C., Hoskins, R.A., et al. (2011a). MiMIC: a
646 highly versatile transposon insertion resource for engineering Drosophila

melanogaster genes. Nat Methods 8, 737-743.
Venken, K.J., Simpson, J.H., and Bellen, H.J. (2011b). Genetic manipulation of genes and cells in the nervous system of the fruit fly. Neuron 72, 202-230.
Vinella, D., Albrecht, C., Cashel, M., and D'Ari, R. (2005). Iron limitation induces SpoT-dependent accumulation of ppGpp in Escherichia coli. Mol Microbiol 56, 958-970.
Wang, B., Dai, P., Ding, D., Del Rosario, A., Grant, R.A., Pentelute, B.L., and Laub, M.T. (2019). Affinity-based capture and identification of protein effectors of the growth regulator ppGpp. Nat Chem Biol 15, 141-150.
Wu, M.N., Joiner, W.J., Dean, T., Yue, Z., Smith, C.J., Chen, D., Hoshi, T., Sehgal, A., and Koh, K. (2010). SLEEPLESS, a Ly-6/neurotoxin family member, regulates the levels, localization and activity of Shaker. Nat Neurosci 13, 69-75.
Wurmthaler, L.A., Sack, M., Gense, K., Hartig, J.S., and Gamerdinger, M. (2019). A tetracycline-dependent ribozyme switch allows conditional induction of gene expression in Caenorhabditis elegans. Nat Commun 10, 491.
Yamada, A., Tsutsumi, K., Tanimoto, S., and Ozeki, Y. (2003). Plant RelA/SpoT homolog confers salt tolerance in Escherichia coli and Saccharomyces cerevisiae. Plant Cell Physiol 44, 3-9.
Yang, X., and Ishiguro, E.E. (2001). Involvement of the N terminus of ribosomal protein L11 in regulation of the RelA protein of Escherichia coli. J Bacteriol 183, 6532-6537.
Yurgel, M.E., Kakad, P., Zandawala, M., Nassel, D.R., Godenschwege, T.A., and Keene, A.C. (2019). A single pair of leucokinin neurons are modulated by feeding state and regulate sleep-metabolism interactions. PLoS Biol 17, e2006409.
Zhang, Y.E., Baerentsen, R.L., Fuhrer, T., Sauer, U., Gerdes, K., and Brodersen, D.E. (2019). (p)ppGpp regulates a bacterial ucleosidase by anaAllosteric two-domain switch. Mol Cell 74, 1239-1249 e1234.
Zhong, G., Wang, H., Bailey, C.C., Gao, G., and Farzan, M. (2016). Rational design of aptazyme riboswitches for efficient control of gene expression in mammalian cells. Elife 5.
Zhou, H., Zheng, C., Su, J., Chen, B., Fu, Y., Xie, Y., Tang, Q., Chou, S.H., and He, J. (2016). Characterization of a natural triple-tandem c-di-GMP riboswitch and application of the riboswitch-based dual-fluorescence reporter. Sci Rep 6, 20871.

682 **FIGURE LEGENDS**

683 **Figure 1. Mesh1 Gene and ppGpp Level in Drosophila**

684 (A) Results of a screen of 1765 P-element insertion lines. The y axis shows sleep
685 latency in minutes and the x axis shows P element insertion lines. Grey shadows
686 showed the standard error of the mean (SEM) from multiple flies of each line,
687 and blue dots and rectangles showed the range of 3-fold of standard deviation
688 from the value of wt. *mesh1-ins* had longer sleep latency than the wt.

689 (B) Results of a screen of 1765 P-element insertion lines. The y axis shows total
690 sleep levels in hours and the x axis shows P element insertion lines. Grey
691 shadows showed SEM from multiple flies of each line, and blue dots and
692 rectangles showed the range of 3-fold of standard deviation from the value of wt.
693 *mesh1-ins* had less total sleep than the wt.

694 (C) Diagrams of *mesh1*-ins and M1KO. In *mesh1*-ins, the P-element was found to be
695 inserted into the CDS of the 1st exon. In M1KO, the entire CDS except the start
696 codon was replaced with stop-2A-attP and 3Px3-RFP. Introns were labeled as
697 straight lines, CDS as unfilled rectangles and untranslated regions (UTRs) as
698 filled rectangles.

699 (D) Statistical analysis of sleep latency. Compared to the wt, *mesh1*-ins exhibited
700 significantly longer sleep latency (Student's t-test, **** denotes $p < 0.0001$).

701 (E) ppGpp metabolism. In *E. coli*, GDP is converted to ppGpp by its synthetase RelA,
702 whereas ppGpp is converted to GDP by the hydrolase SpoT. In *D. melanogaster*,
703 only the hydrolase Mesh1 has been discovered but the synthetase is unknown.

704

Figure 2. Identification and Quantitative Analysis of ppGpp in Drosophila

(A-C) UPLC-MS profiles of standard ppGpp (A), wt fly extracts (B), and M1KO fly extracts (C). Horizontal axis is time (minutes), and vertical axis is intensity of MS signal at m/z = 601.95, which corresponds to standard ppGpp (A).

(D-E) Statistical analyses of ppGpp measurements under fed (D) or starved (E) conditions in *Drosophila*. For each genotype, approximately 2000 male flies were sacrificed for UPLC-MS measurements. In both fed and starved conditions, compared to that in wt, ppGpp level was significantly increased in M1KO (Student's t-test, **** denoting $p < 0.0001$).

(F) Mesh1 protein expressed in E.coli was purified and added into extracts from M1KO flies. ppGpp in the extracts was reduced by Mesh1.

(G-H) Statistical analyses of ppGpp measurements under fed (D) or starved (E) conditions in germ-free Drosophila. Germ-free flies were generated and amplified (see method in details), and in each condition 2000 male flies were sacrificed for measurement by UPLC-MS.

Figure 3. Sleep Phenotypes in M1KO Mutant Flies

(A) Profiles of sleep and awakening in M1KO Flies. Rest time for every 30 min was plotted (with the SEM as the error bars). Compared to the wt flies, M1KO flies began sleep later and wake up earlier. Dusk (ZT 0-3) and dawn (ZT 9-12) of night time sleep were denoted with green bars.

(B-D) Statistical analyses of sleep level during night time (B), day time (C) or in total

(D). Compared to the wt, M1KO flies slept significantly less at night (Student's t-test, **, **** denoting $p < 0.01$, and $p < 0.0001$ respectively).

(E-F) Statistical analyses of sleep latency during night time (E), or day time (F). Compared to the wt, M1KO flies exhibited a significant increase in night sleep latency (Student's t-test, **** denoting $p < 0.0001$).

(G-H) Statistical analyses of summed awakening numbers at dusk (G, ZT0-3) and dawn (H, ZT9-12) shown in (A). Awakening numbers of both dusk and dawn were significantly increased in M1KO flies (Student's t-test, **** denoting $p < 0.0001$).

Figure 4. Significance of the Hydrolysis Activity of Mesh1 in Drosophila Sleep

(A) Diagrams of constructs used to generate M1KO and M1KOGal4 flies. *mesh1* CDS except the start codon was deleted in both M1KO and M1KOGal4, and the only difference is that a T2A-fused Gal4 (with a stop codon) were placed in M1KOGal4.

(B) Statistical analyses of sleep latency at night. Columns 1-3: wt, M1KOGal4/+ and M1KOGal4/M1KOGal4 flies, with the sleep latency significantly increased in M1KOGal4/M1KOGal4 (Column 3). Columns 4-5: M1KOGal4/M1KO and M1KOGal4/+. Columns 6-8: M1KOGal4/M1KO > UAS-Mesh1/+, M1KO/M1KO, UAS-Mesh1/+, M1KOGal4/+>UAS-Mesh1/+. M1KOGal4/M1KO>UAS-Mesh1 (Column 6) could fully rescue the sleep latency phenotype (Columns 7-8). Columns 9-11: M1KOGal4/M1KO>UAS-Mesh1E66A/+, M1KO/M1KO, UAS-Mesh1E66A/+, M1KOGal4/+>UAS-Mesh1E66A/+. The hydrolysis-deficient line UAS-Mesh1E66A/+ driven by M1KOGal4/M1KO (Column 9) failed to rescue sleep

latency (Columns 10-11). Comparison was based on two-way ANOVA and Bonferroni post-tests with **** denotes $p < 0.0001$.

(C) Statistical analyses of awakening number at dusk. Columns 1-3: awakening number significantly increased in M1KO (Column 3). Columns 4-5: M1KOGal4/M1KO (Column 4) had more awakening number than the wt. Columns 6-8: M1KOGal4/M1KO > UAS-Mesh1 (Column 6) could rescue the awakening number deficiency (Columns 7-8). Columns 9-11: the hydrolysis-deficient UAS-Mesh1E66A/+ driven by M1KOGal4/M1KO (Column 9) failed to rescue the awakening number deficiency (Columns 10-11).

(D) Statistical analyses of awakening number at dawn.

Figure 5. The Expression Pattern of M1KOGal4

(A) Neurons expressing mCD8-GFP driven by M1KOGal4 in the brain (left) and the VNC (right). Magenta showed immunostaining by the nc82 monoclonal antibody specific for neurons.

(B) Nuclei expressing red-stinger driven by M1KOGal4 in the brain (left) and the VNC (right). Redstinger is presented in green.

(C) Dendrites revealed by M1KOGal4>UAS-denmark in the brain (left) and the VNC (right). The dendritic marker denmark is presented in green.

(D) Synaptic terminals revealed by M1KOGal4>UAS-Syt.eGFP in the brain (left) and the VNC (right). Syt.eGFP is presented in green.

(E) A diagrammatic summary of neurons revealed by M1KOGal4. A: anterior sections.

771 P: posterior sections.

772

773 **Figure 6. Effects of RelA Expression on Drosophila Sleep**

774 (A) Statistical analyses of sleep latency when RelA was expressed in all cells with
775 (tub-Gal4), neurons (elav-Gal4), glia (repo-Gal4) or mesh1 positive cells
776 (mesh1Gal4). (1) wt , (2) M1KO, (3) UAS-RelA/+, (4) M1KOGal4/+>UAS-RelA/+,
777 (5) M1KOGal4/+, (6) elav-Gal4/+> UAS-RelA/+, (7) elav-Gal4/+, (8)
778 repo-Gal4/+>UAS-RelA/+, (9) repo-Gal4/+, (10) tub-Gal4/+>UAS-RelA/+, (11)
779 tub-Gal4/+. Comparisons were based on two-way ANOVA and Bonferroni post-tests
780 with **** denoting $p < 0.0001$.

781 (B) Statistical analyses of awakening number at dusk when RelA was expressed in all
782 cells (10), neuron (6), glia (8) or *mesh1* positive cells (4).

783 (C) Statistical analyses of sleep latency with RelA expression in different subsets of
784 PI neurons. (1) wt, (2) M1KO, (3) UAS-RelA/+, (4) c767/+>UAS-RelA/+, (5)
785 c767/+, (6) Dh44-Gal4/+>UAS-RelA/+, (7) Dh44-Gal4/+, (8) Dilp2-Gal4/+>
786 UAS-RelA/+, (9) Dilp2-Gal4/+, (10) SIFa2-Gal4/+>UAS-RelA/+, (11) SIFa2-Gal4/+,
787 (12) R19610-Gal4/+>UAS-RelA/+, (13) UAS-RelA/+. Comparisons were based on
788 two-way ANOVA and Bonferroni post-tests, with **, ***, **** denoting $p < 0.01$, p
789 < 0.001, $p < 0.0001$ respectively.

790 (D) Statistical analyses of awakening number with RelA expression in different
791 subsets of PI neurons. Comparisons were based on two-way ANOVA and Bonferroni
792 post-tests with **, ***, **** denoting $p < 0.01$, $p < 0.001$, $p < 0.0001$ respectively.

Figure 7. Effects of Mesh1 Overexpression on Drosophila Sleep

(A) Statistical analyses of sleep latency when Mesh1 was overexpressed in all cells, neurons, glia or *mesh1* positive cells. (1) wt, (2) M1KO, (3) UAS-Mesh1/+, (4) M1KOGal4/+ > UAS- Mesh1/+, (5) M1KOGal4/+, (6) elav-Gal4/+ > UAS- Mesh1/+, (7) elav-Gal4/+, (8) repo-Gal4/+>UAS-Mesh1/+, (9) repo-Gal4/+, (10) tub-Gal4/+, UAS-Mesh1/+, (11) tub-Gal4/+. Comparisons were based on two-way ANOVA and Bonferroni post-tests with **, *** denoting $p < 0.01$ and $p < 0.001$ respectively.

(B) Statistical analyses of awakening number when Mesh1 was overexpressed in all cells, neurons, glia or *mesh1* positive cells. Comparisons were based on two-way ANOVA and Bonferroni post-tests with *** and **** denoting $p < 0.001$ and $p < 0.0001$ respectively.

(C) Representative sleep profiles for lines in (A) and (B). Red arrow denotes sleep latency at dusk. UAS-Mesh1/+ in the top and bottom panels was the shared control, with the top panel showing that repo-Gal4>UAS Mesh1 did not affect sleep latency whereas the bottom panel showing that elav-Gal4>UAS Mesh1 shortened sleep latency.

(D) Statistical analyses of sleep latency with Mesh1 overexpression in different PI subsets. (1) wt, (2) M1KO, (3) UAS-Mesh1/+, (4) c767-Gal4/+ and UAS-Mesh1/+, (5) c767-Gal4/+, (6) Dh44-Gal4/+ and UAS-Mesh1/+, (7) Dh44-Gal4/+, (8) Dilp2-Gal4/+ and UAS-Mesh1/+, (9) Dilp2-Gal4/+, (10) SIFa2-Gal4/+ and UAS-Mesh1/+, (11) SIFa2-Gal4/+, (12) R19G10-Gal4/+ and UAS-Mesh1/+, (13)

R19G10-Gal4/+. Comparisons were based on two-way ANOVA and Bonferroni post-tests with **, ***, **** denoting $p < 0.01$, $p < 0.001$ and $p < 0.0001$ respectively.

(E) Statistical analyses of awakening number with Mesh1 overexpression in different PI subsets. Comparisons were based on two-way ANOVA and Bonferroni post-tests with *, **, *** denoting $p < 0.05$, $p < 0.01$ and $p < 0.001$ respectively.

(F) Representative sleep profiles for lines in (D) and (E). Red arrow denotes sleep latency at dusk. Note that the UAS-Mesh1/+ profile in the top and bottom panels was the shared control, with the top panel showing that Dh44-Gal4>UAS Mesh1 did not affect sleep latency whereas the bottom panel showing that Dilp2-Gal4>UAS Mesh1 shortened sleep latency.

Figure 8. Effects of Mesh1 Knockout Mutations or RelA Expression on SISL

(A) SISL in M1KO. Baseline sleep was recorded on food for 3 days (recording at day 2 and day 3), before flies were transferred to 1% agar at the end of the 3rd day, followed by sleep recording while starvation of 24hr.

(B) Statistical analysis of SISL in (A). Sleep was lost ~10% at night and ~50% at day, compared to the baseline in wt. This was significantly exacerbated in M1KO at night (Student's t-test with *** denoting $p < 0.001$).

(C) Statistical analyses of SISL with Mesh1 and Mesh1E66A rescue experiments. (1) wt, (2) M1KO/+, (3) M1KO/M1KO, (4) M1KOGal4/M1KO, (5) M1KOGal4/+, (6) M1KOGal4/M1KO and UAS-Mesh1/+, (7) M1KO/M1KO and UAS-Mesh1/+, (8)

837 M1KOGal4/+ and UAS-Mesh1/+, (9) M1KOGal4/M1KO and UAS-Mesh1E66A/+,
838 (10) M1KO/M1KO and UAS-Mesh1E66A/+, (11) M1KOGal4/+ and
839 UAS-Mesh1E66A/+. Comparison was based on two-way ANOVA and Bonferroni
840 post-tests with **, *** denoting $p < 0.01$, $p < 0.001$ respectively.
841 (D) Statistical analyses of SISL with RelA expression in all cells, neurons, glia or
842 *mesh1* positive cells. (1) wt, (2) M1KO, (3) UAS-RelA/+, (4) M1KOGal4/+>
843 UAS-RelA/+, (5) M1KOGal4/+, (6) elav-Gal4/+>UAS-RelA/+, (7) elav-Gal4/+, (8)
844 repo-Gal4/+>UAS-RelA/+, (9) repo-Gal4/+, (10) tub-Gal4/+>UAS-RelA/+, (11)
845 tub-Gal4/+. Comparisons were based on two-way ANOVA and Bonferroni post-tests
846 with **** denoting $p < 0.0001$.
847 (E) Statistical analyses of SISL with RelA expressing in different subsets of PI. (1)
848 wt, (2) M1KO, (3) UAS-RelA /+, (4) c767-Gal4/+ and UAS-RelA /+, (5)
849 c767-Gal4/+ (6) Dh44-Gal4/+ and UAS-RelA /+, (7) Dh44-Gal4/+, (8) Dilp2-Gal4/+
850 and UAS-RelA/+,(9) Dilp2-Gal4/+, (10) SIFa2-Gal4/+ and UAS-RelA/+, (11)
851 SIFa2-Gal4/+, (12) R19G10-Gal4/+ and UAS-RelA/+, (13) R19G10-Gal4/+.
852 Comparison was based on t-test with *** denoting $p < 0.001$.
853

854 **Figure 9. Effect of Mesh1 Overexpression of on SISL**

855 (A) Statistical analyses of SISL with Mesh1 overexpression in neurons or other cells.
856 (1) wt, (2) M1KO, (3) UAS-Mesh1/+, (4) M1KOGal4/+>UAS-Mesh1/+, (5)
857 M1KOGal4/+, (6) elav-Gal4/+>UAS-Mesh1/+, (7) elav-Gal4/+, (8)
858 repo-Gal4/+>UAS- Mesh1/+, (9) repo-Gal4/+, (10) tub-Gal4/+>UAS-Mesh1/+

tub-Gal4/+ (11). Comparisons were based on two-way ANOVA and Bonferroni post-tests with ***, **** denoting $p < 0.001$, $p < 0.0001$ respectively.

(B) Statistical analyses of SISL with Mesh1 overexpression in different subsets of PI. (1) wt, (2) M1KO, (3) UAS-Mesh1/+, (4) c767-Gal4/+>UAS-Mesh1/+, (5) c767-Gal4/+, (6) Dh44-Gal4/+>UAS-Mesh1/+, (7) Dh44-Gal4/+, (8) Dilp2-Gal4/+> UAS-Mesh1/+, (9) Dilp2-Gal4/+, (10) SIFa2-Gal4/+>UAS-Mesh1/+, (11) SIFa2-Gal4/+, (12) R19G10-Gal4/+>UAS-Mesh1/+, (13) R19G10-Gal4/+. Comparison was based on t-test with *** denoting $p < 0.001$.

(C) Representative sleep profiles of SISL in (A). Baseline sleep in black, and sleep during starvation in blue. Black arrows indicate that night SISL is not significantly different from wt; red arrows indicate SISL phenotype similar to that in M1KO.

(D) Representative sleep profiles of SISL in (B).

Figure S1. Quantifications: Mesh1 RNA and ppGpp

(A) Examination of germ-free status by growing bacteria on LB plate. 6 conditions were examined: (1) blank: direct incubation of LB plate; (2) water germ-: strike LB plate with germ-free water; (3) wt germ-: extract germ-free wt flies with germ-free water, and strike LB plate with the extract; (4) M1KO germ-: extract germ-free M1KO flies with germ-free water, and strike LB plate with the extract; (5) wt germ+: extract normal wt flies with germ-free water, and strike LB plate with the extract; (6) M1KO germ+: extract normal M1KO flies with germ-free water, and strike LB plate with the extract. Among these conditions, bacteria only appear on plates of wt germ+

and M1KO germ+.

(B) Examination of germ-free status by 16S rDNA PCR. 5 pairs of 16S PCR primers (denoted as pm) were used, including (1) 16S-27F/16S-519R; (2) 16S-357F/16S-907R; (3) 16S-530F/16S-1110R; (4) 16S-926F/16S-1492R; (5) 16S-1114F/16S-1525R. The upper and lower bands at marker lane (Trans2K) correspond to 500bp and 250bp. PCR signals by pm1, pm3 and pm5 were detected in both controls (wt germ+ and M1KO germ+), while no signals were detected in all three germ-free groups (water germ-, wt germ-, M1KO germ-).

(C) Measurement of Mesh1 RNA by quantitative polymerase chain reaction (qPCR). $Log_{10}(RQ)$ is the log form of relative quantity of Mesh1 mRNA in Drosophila. (1) M1KO/+, (2) *mesh1*-ins, (3) M1KO, (4) M1KOGal4/M1KO, (5) M1KOGal4/M1KO and UAS-Mesh1/+, (6) M1KO/M1KO and UAS-Mesh1/+, (7) M1KOGal4/+, UAS-Mesh1/+, (8) M1KOGal4/+ and UAS-Mesh1/UAS-Mesh1, (9) M1KOGal4/+.

(D) Diagrams of the ppGpp synthetase domain (SD) and the hydrolase domain (HD) in RSH proteins from E. coli, D. melanogaster, and H. sapiens. The mammalian hddc3 and the Drosophila Mesh1 proteins contain only HD, the bacterial RelA protein contains a weak HD, an active SD and a regulatory domain (RD). Bacterial SpoT contains an active HD, a weak SD and a RD.

(E) Standard curve of MS peak area to ppGpp concentration. x-axis is log2 value of standard ppGpp concentration (nM), and y-axis is log2 value of peak area of MS signal.

(F) Measurement of ppGpp in vitro. Blank is the mixture of reaction buffer, GDP and

903 ATP. Standard ppGpp is a commercial sample. RelA+GDP is the addition of purified
904 RelA to the mixture of reaction buffer, GDP and ATP. Mesh1+ppGpp is the standard
905 ppGpp plus purified Mesh1. Mesh1E66A+ppGpp is the standard ppGpp plus the
906 mutant protein Mesh1E66A expressed in *E. coli* and purified.
907 (G) Measurement of ppGpp level in vivo. (1) M1KO/+, (2) M1KO, (3) M1KOGal4/+,
908 (4) M1KOGal4/M1KO and UAS-Mesh1/+, (5) M1KOGal4/+ and UAS-Mesh1/+, (6)
909 M1KOGal4/M1KO and UAS-Mesh1E66A/+, (7) M1KOGal4/+ and
910 UAS-Mesh1E66A/+.
911

912 **Figure S2. Phenotypic Analyses of Sleep and Circadian Rhythm**
913 (A) Sleep analysis under LD condition. Nighttime bout number and bout length (in
914 filled boxes on the left) and daytime bout number and bout length (unfilled boxes on
915 the right) were not significantly different between the wt and the M1KO flies.
916 (B) Sleep and awakening number profiles under DD condition.
917 (C-I) Sleep analyses under DD conditions. Sleep level at presumptive night (C), at
918 presumptive day (D), total sleep level (E), awakening number at dusk (H), at dawn (I),
919 sleep latency at presumptive night (F), at presumptive day (G).
920 (K-L) Periodic length (K) and rhythmicity strength Qp (L) of wt and M1KO flies.
921 (L) Circadian profiles of wt flies under the LD and DD conditions.
922 (M) Circadian profiles of M1KO flies under the LD and DD conditions.
923

924 **Figure S3. A Functional Screen of CCT-Gal4 Lines**

(A) A pilot screen of sleep latency with 102 CCT-Gal4 lines driving RelA expression. Candidates above blue line showing three standard deviations away from the mean. 6 Gal lines were found to be able to increased sleep latency significantly: Capa-R, CCHa2-R, LkR, OA2, CG13229 and Trh.

(B-G) mCD8-GFP expression driven by each of the CCT Gal4 lines: Capa-R (B), OA2 (C), CCHa2-R (D), CG13229 (E), LkR (F) and Trh (G). PI neurons were observed in all these lines.

Figure S4. Expression Examined by Intersection with Mesh1

(A) Diagram of M1KIflp. The CDS after the start codon of *mesh1* gene was replaced by 2A-flp-3Px3-RFP. This is similar to Mesh1Gal4 but with Flp in place of Gal4. This line was used to intersect with Gal4 lines from the CCT screen (Capa-R, CCHa2-R, LkR, OA2, CG13229 and Trh). Each was indeed expressed in Mesh1 positive PI neurons. Shown from B to D are examples.

(B-D) The UAS-FRT-stop-FRT-mCD8-GFP expression patterns of M1KIflp and PI-Gal4 intersection lines. Insets show higher magnification views of the PI.

(E) An anti-Dilp2 antibody was used in immunostaining in M1KOGal4>UAS-mCD8-GFP flies and showed Mesh1 positive neurons to be also positive for Dilp2.

Figure S5. Sleep profiles of rescue lines in SISL

(A-K) baseline sleep is shown in black, and sleep during starvation shown in blue;

947 black arrows indicate that night SISL is not significantly changed compared to wt or
948 corresponding parental controls; red arrows indicate that a specific genotype
949 phenocopied M1KO in SISL.

950

951 **Figure S6. Sleep Latency in SISL**

952 Sleep latency (A, C) at night or day (B, D). A and B are before starvation, whereas C
953 and D are during starvation.

954 **Supplementary Table S1. Primers for PCR, qPCR and Genotyping**

955 **Supplementary Table S2. Standard Curve Data of MS peak area to ppGpp**
956 **concentration.**

957

958 **EXPERIMENTAL PROCEDURES**

959 **Fly Stocks and Rearing Conditions**

960 All flies were reared on standard corn meal at 25℃ and 60% humidity, under
961 12hr:12hr LD cycle (unless specified otherwise). Before behavioral assays, stocks
962 were backcrossed into the background of an isogenized Canton S wt line in the lab for
963 7 generations (Zhou, Rao and Rao, 2008).

964 Lines ordered from the Bloomington Stock Center included: 47887
965 (R19G10-Gal4), 30848 (c767-Gal4), 51987 (Dh44-Gal4), nos-phiC31, 37516
966 (Dilp2-Gal4), 5137 (UAS-mCD8-GFP). SIFa-Gal4 was a gift from Dr. J. Veenstra
967 (University of Bordeaux). P-element insertion lines were a gift from Dr. U Heberlein,
968 and CCT-Gal4 library was a collection previously generated in our lab (Deng *et al*.,
969 2019). isoCS and w^{1118} were wild-type and white-eye wild-type lines.

970

971 **Reagents and Plasmids**

972 PCR was performed with Phanta-Max Super-Fidelity DNA Polymerase (Vazyme).
973 Genotyping PCR was performed with 2x Taq PCR StarMix with Loading Dye
974 (GenStar). Restriction enzymes KpnI-HF, SacII, NotI-HF, XbaI, XhoI, BamHI-HF,
975 DpnI, EcoRI-HF and XbaI were from New England BioLabs. Total RNA was
976 extracted from flies with RNAprep pure Tissue Kit (TIANGEN). Reverse
977 transcription for cDNA cloning was performed with PrimeScript^{TM} II 1st Strand cDNA
978 Synthesis kit (Takara), Gibson assembly was performed with NEBuilder HiFi DNA
979 Assembly Master Mix. Transformation for cloning was performed with Trans-5 α
980 (TransGen), and transformation for expression was performed with Transetta
981 (TransGen). BL21 (TransGen) was used as the bacterial gene template. Reverse
982 transcription for quantitative PCR (qPCR) analyses was performed with PrimeScript
983 RT Master Mix kit (Takara). qPCR was performed with TransStart Top Green qPCR
984 SuperMix kit (TransGen).

985 pACU2 was a gift from Drs. Lily and YN Jan. The plasmids previously used in
986 our lab included: pBSK, pET28a+. Templates of STOP-attP-3Px3-RFP,
987 T2A-Gal4-3Px3-RFP, and T2A-flp-3Px3-RFP were previously generated in the lab
988 (Deng *et al*., 2019).

989

990 **Molecular Cloning and Generation of Genetically Modified Flies**

991 Generation of all KO and KI lines was based on the CRISPR-Cas9 system with

992 homologous recombination, according to previous procedures described (Ren *et al*.,
993 2013). U6b vector was used for the transcription of sgRNA (Ren *et al*., 2013) and
994 construction of targeting vectors were based on previous procedures in our lab (Deng
995 *et al*., 2019).

996 To generate KO lines, a mixture of two U6b-sgRNA plasmids and one targeting
997 vector was injected into Drosophila embryos. To generate U6b-sgRNA, two sgRNAs
998 were selected on website (https://www.flyrnai.org/crispr), and designed into a pair of
999 primers (M1KOSgRNA-F and M1KOSgRNA-R) without PAM sequence. The other
1000 pair of primers (U6b-laczrv and U6b-primer1) were designed on the backbone of U6b
1001 vector, so that they could generate PCR products containing two parts of U6b (shorter
1002 fragment by M1KO sgRNA-F and U6b-laczrv, longer fragment by M1KO sgRNA-R
1003 and U6b-primer1), which shared overlapping sequences in both ends. U6b-sgRNA
1004 plasmid was built by Gibson-assembly of the PCR products. To generate the targeting
1005 vector, two fragments (2kbps) flanking the entire CDS of gene *mesh1* except start
1006 codon were cloned as 5'Arm (PCR with primers M1KO5F and M1KO5R) and 3'Arm
1007 (PCR with primers M1KO3F and M1KO3R). Vector pBSK was digested with *KpnI*
1008 and *SacII*, and the PCR products were introduced into the digested pBSK by
1009 Gibson-assembly. New restriction sites (*NotI* and *XhoI*) were introduced between the
1010 two arms for further use. To generate a targeting vector for M1KO, the fragment
1011 STOP-attP-3Px3-RFP was cloned with primers attP2M1KOF and attP2M1KOR, and
1012 inserted between *NotI* and *XhoI* by Gibson-assembly; and for M1KOGal4,
1013 T2A-Gal4-3Px3-RFP was inserted at same location. A mixture of U6b-sgRNA and

the targeting vector was injected into embryos of *nano*-Cas9 or *vasa*-Cas9 (Ren *et al*., 2013). F1 individuals of RFP+ eyes were collected after being crossed with w^{1118} flies.

To generate KI line M1KIflp, similar procedures were performed. For U6b-sgRNA, primers for shorter fragment were M1KISgRNA-F and U6b-laczrv, while primers for longer fragment were M1KIsgRNA-R and U6b-primer1. For the targeting vector, PCR for 5'Arm was performed with M1KI5F and M1KI5R, and 3'Arm with M1KI3F and M1KI3R. The site flanked by two arms was selected near the very end of *mesh1* CDS, so that the stop codon was removed and the CDS was fused with T2A-flp-3Px3-RFP with primers flp2M1KIF and flp2M1KIR.

Generation of transgenic UAS lines was based on vector pACU2 (Han, Jan and Jan, 2011). Drosophila cDNA was generated by reverse transcription from total RNA. By using the cDNA as template, *mesh1* CDS was amplified with primers (M1CDSF and M1CDSR), and inserted into digested pBSK (by *EcoRI* and *KpnI*). Point mutation of *mesh1*E66A was generated on this plasmid with primers M1E66AF and M1E66AR. Both *mesh1* CDS and Mesh1E66A were cloned with primers M1ACU2F and M1ACU2R. RelA sequence was cloned from BL21 bacteria with primers RAACU2F and RAACU2R. All the above were inserted into digested pACU2 (*EcoRI* and *XbaI*) by Gibson assembly. pACU2 constructs were inserted into attP2 by nos-phiC31 during embryo injection.

All fly stocks were confirmed by PCR and qPCR, and primers were shown in Supplementary Table S1.

1036

1037 **Molecular Cloning and Inducible Expression in Bacteria**

1038 pET28a+ was used for bacterial expression of Mesh1 and RelA proteins. *mesh1* CDS
1039 and *mesh1*E66A were generated with primers M1ET28F and M1ET28R. RelA was
1040 cloned from BL21 bacteria with primers RAET28F and RAET28R. All the above
1041 were inserted into pET28a+ by Gibson assembly. Competent cells transformed with
1042 the above constructs were amplified for inducible expression. To induce expression, a
1043 colony was inoculated into 1ml kanamycin containing Luria broth (LB) media, and
1044 incubated at 37℃ for 2 hr. 800µl was transferred into a flask with 800ml kanamycin+
1045 LB media and incubated for ~3hr at 37℃ 220rpm, until OD_{600} was 0.5 to 0.6. 800µl
1046 1M isopropyl β-D-1 thiogalactopyranoside (IPTG) was added into the flask. For RelA,
1047 the induction was at 37℃ for 3hr; for Mesh1 and Mesh1E66A, it was at 16℃ for 16
1048 hr. Bacteria was harvested by centrifugation followed by lysis with ultrasonication
1049 (Power: 30%, lysis 2s, wait 2s, 30 cycles) and centrifugation. Supernatants were
1050 passed through nickle columns, followed by two times of wash with 10ml binding
1051 buffer (20mM Tris-HCl pH 7.4, 0.5M NaCl, 5mM imidazole), and elution with 5ml
1052 elution buffer (20mM Tris-HCl pH7.4, 0.5M NaCl, 500mM imidazole). Each step
1053 was monitored on 10% SDS-PAGE to check protein expression. Eluted protein was
1054 enriched in Millipore Amicon Ultra-15, and re-suspended in 1ml of protein storage
1055 buffer (20mM Tris-HCl pH7.4, 150mM NaCl, 0.3% CHAPS, 1mM DTT).

1056

1057 **Generation of Germ-Free Flies**

Replace the sponge of bottle containing standard fly medium with autoclavable PP bag, and autoclave twice. Evaporate water of food surface in laminar hood and under UV light for 1 hour.

According to previous report (Kietz, Pollari and Meinander 2018), prepare a simple device for Drosophila egg collection and filter for egg wash, and use the device to collect fly eggs for 5 hours, while filters were soaked in 75% EtOH overnight.

Prepare 5x 50ml centrifuge tubes, filled with the following solutions: A. 3.3% Walsh hand-sanitizer; B. 75% EtOH; C. 1% active chlorine; D. 0.1% TritonX-100 + 1xPBS; E. sterilized ddH2O.

Use cell scraper to collect eggs onto filters, and wash filters from A to E, and disperse the resuspended eggs onto autoclaved fly medium.

Keep rearing at clean incubator for 20 days, and amplify the generated germ-free flies.

Extraction and Measurement of ppGpp

To extract ppGpp from *Drosophila*, 24ml formic acid was added into about every 2000 flies. After grinding 10,000 rpm for 15 seconds, 3ml 30% tri-chloric acetic acid was added to precipitate proteins. The above procedures were repeated to collect extracts if necessary. Supernatants were enriched with SPE column (Waters Oasis 6cc WAX), and effluent was titrated and lyophilized overnight, and powders were re-suspended with 200μl water.

To measure the level of ppGpp, ZORBAX Eclipse XDB-C18 2.1x100mm column was used in UPLC-MS (Thermo ULtiMate 3000, and Thermo QE HF-X),

according to a modified version of previous method (Ihara, Ohta and Masuda, 2015). The mobile phase included: Buffer A (8mM *N*,*N*-dimethylhexylamine, 160µl acetic acid, 500ml water) and Buffer B (Acetonitrile). The UPLC program was: at 0min, A:B = 100%:0%; at 10min, A:B = 40%:60%, with linear increment; at 10.01-14min, keep A:B = 0%:100%; at 14.01-18min, keep A:B=100%:0%. The m/z of ppGpp should be 601.95, and fly number was used for normalization.

Behavioral Assays

To analyze baseline sleep under 12hr:12hr LD cycles, approximately 48 flies of each genotype were loaded into glass tubes for video tracing (fps=1), which was analyzed by an in-house software as described previously (Qian *et al*., 2017; Dai *et al*., 2019; Deng *et al*., 2019). Continuous immobility of >5min was defined as a sleep bout (Hendricks *et al*., 2000, Shaw *et al*., 2000). Sleep latency at dusk was defined as the that from light-off to the point when the 1st sleep bout appeared.

To analyze the circadian rhythm, activities under 12hr:12hr LD cycles were recorded for 7 days, which was then computed by ActogramJ (Schmid *et al*., 2011). Period was calculated by periodogram of Chi-square, and rhythmicity was assessed with Qp.

To analyze awakening numbers, video tracing data was converted to data of simulated cross-beam. In the simulation, the middle line for each tube was set as the virtual beam. According to a previous study (Tabuchi *et al*., 2018), brief awakening was defined as 1 cross per min, and the awakening number was the sum of such

events in every 30 min. Awakening number of dusk was the sum of brief awakenings at ZT0-3, and awakening number of dawn was the sum of brief awakenings at ZT9-12.

To test starvation-induced sleep loss (SISL), sleep was recorded for the first 3 days (3rd day defined as baseline), and flies were quickly transferred to 1% agar at the end of the light phase of 3rd day, followed by a 24 hr recording of sleep during starvation. SISL ratio was defined as (starvation sleep-baseline sleep)/ baseline sleep.

Immunohistochemistry and Imaging

To prepare flies for imaging, 5 flies per genotype were dissected in phosphate-buffered saline (PBS). Dissected tissues were transferred to a tube of 400µl 2% PFA, and fixed for 55 min. Tissues were washed 3 times with 400µl brain wash buffer (PBS containing 1% TritonX-100, 3% m/V NaCl), and then transferred to 400µl blocking buffer (PBS containing 2% TritonX-100, 10% normal goat serum), followed by incubation at 4℃ overnight. Tissues were transferred to dilution buffer (0.25% TritonX-100, 1% NGS, 1x PBS) and added with primary antibodies including, 1:1000 chick anti-GFP (Abcam) and 1:40 mouse anti-nc82 (DSHB). Tissues were stained at 4℃ overnight, followed by 3 washes with 400µl brain wash buffer. Samples were transferred to fresh dilution buffer containing secondary antibodies including, 1:200 Alexa Fluor goat anti-chick 488 (Invitrogen) and 1:200 Alexa Fluor goat anti-mouse 633 (Invitrogen), followed by 3 washes with 400µl brain wash buffer.

To prepare for imaging, samples were placed into a drop of Focus Clear (Cell

Explorer Labs, FC-101), which was restricted by a piece of paper circle on a glass slide. Samples were visualized on Zeiss LSM 710 confocal microscope.

CONTACT FOR REAGENT AND RESOURCE SHARING

Further information and requests for resources and reagents should be directed to and will be fulfilled by the Lead Contact, Yi Rao (yrao@pku.edu.cn).

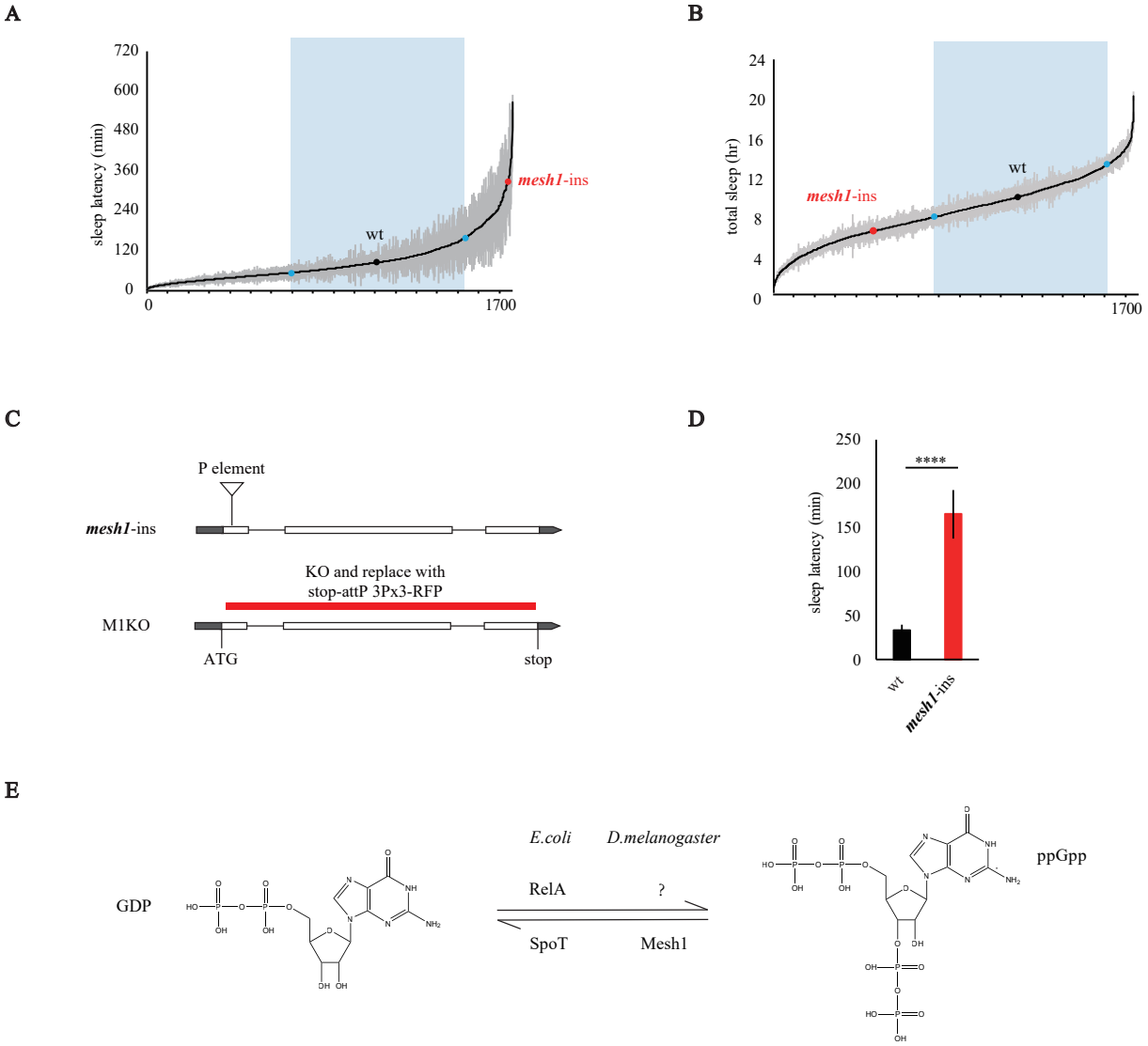

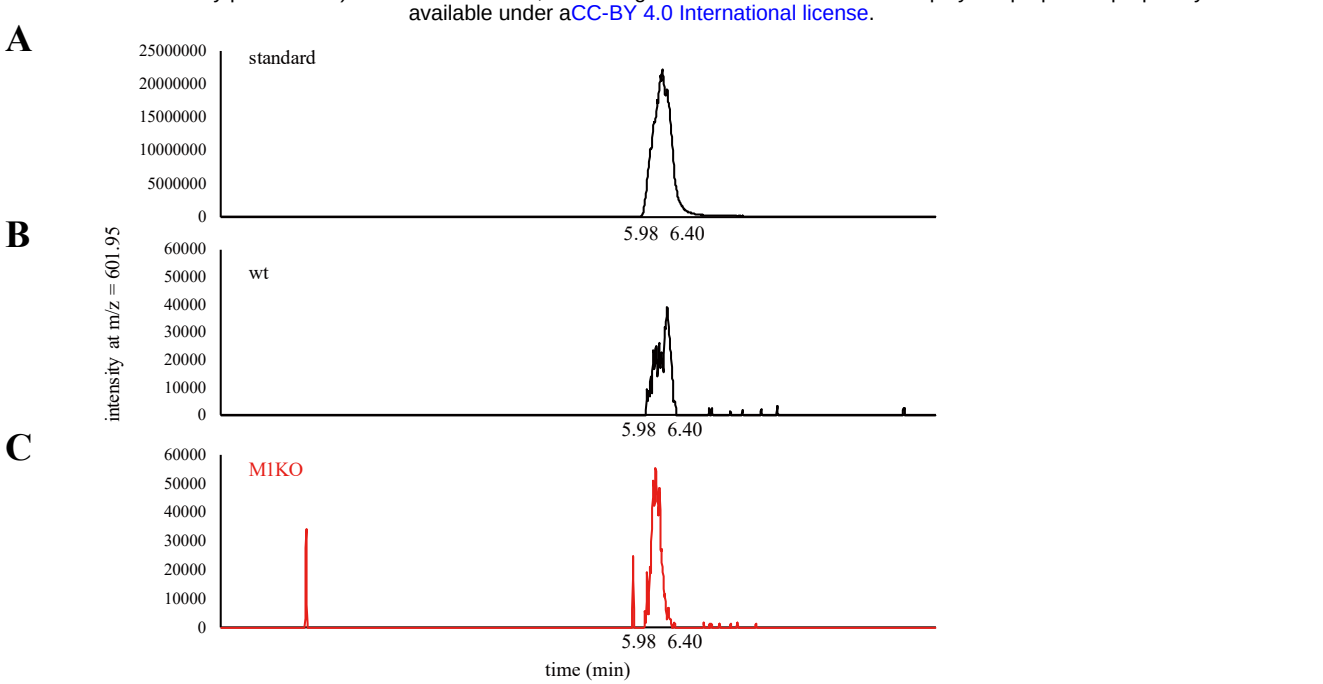

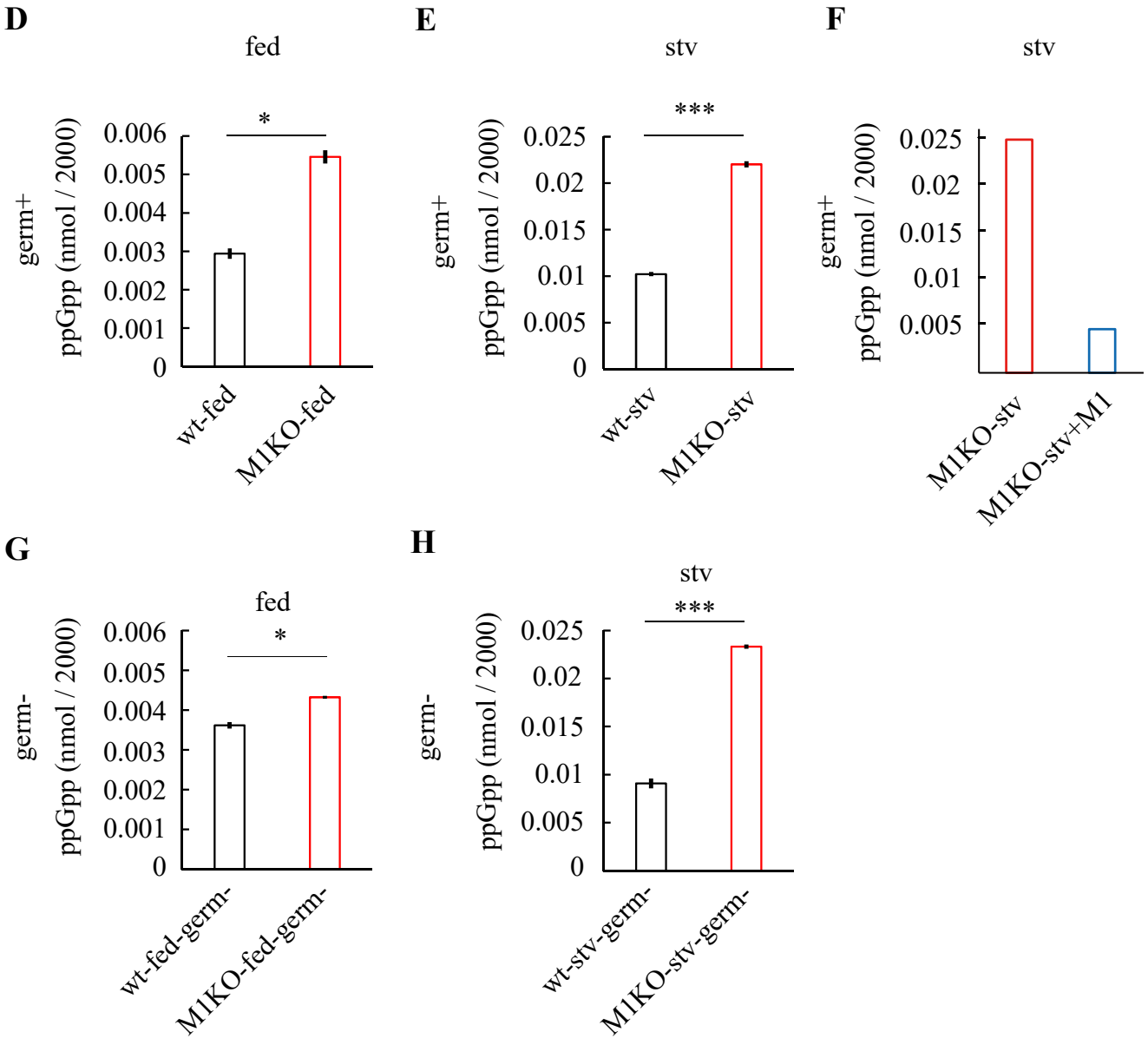

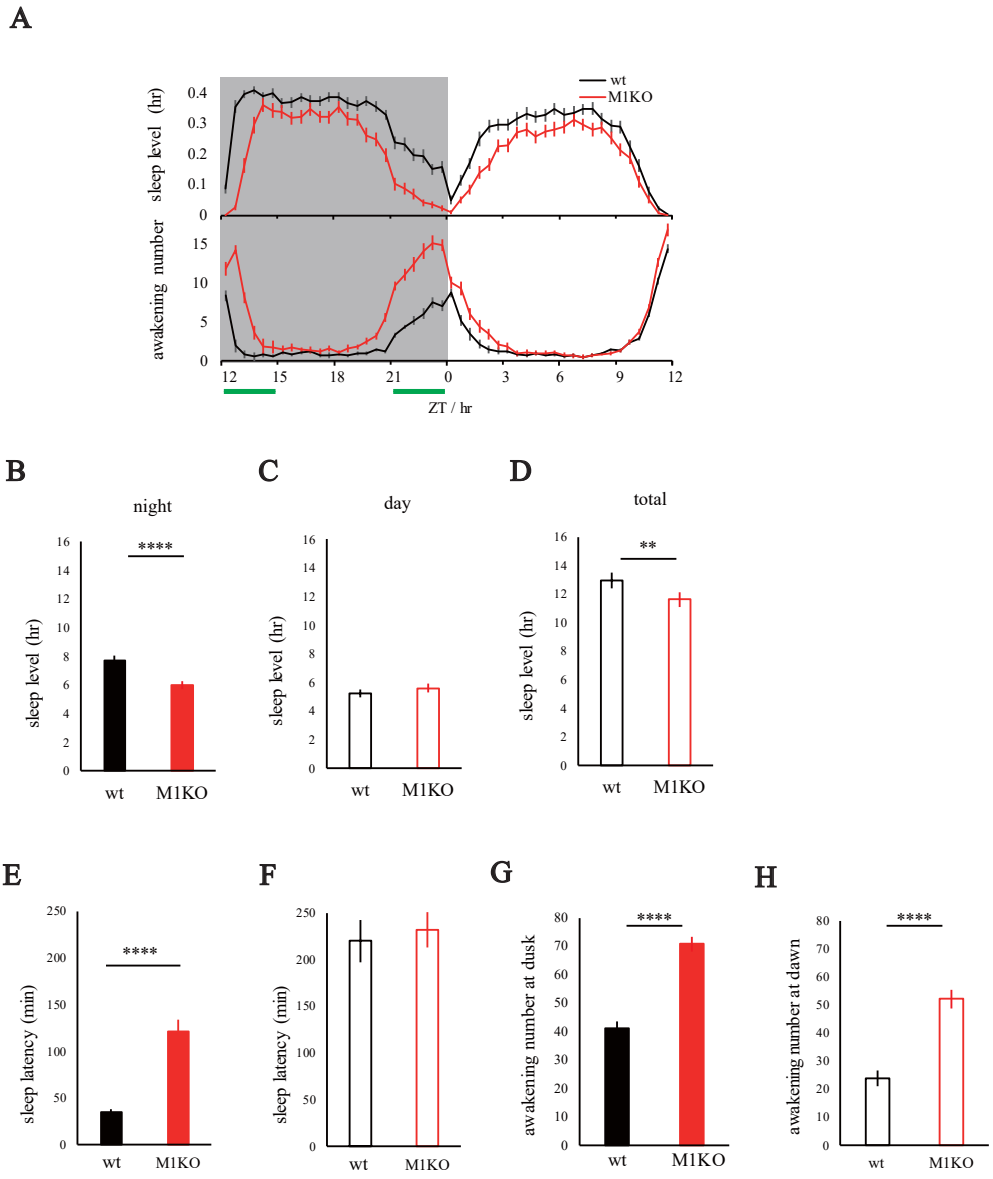

A

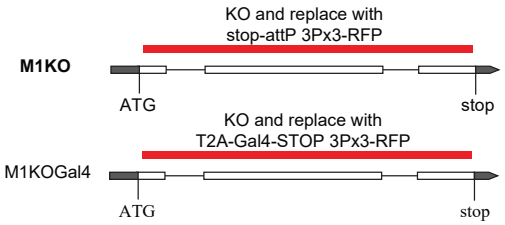

B

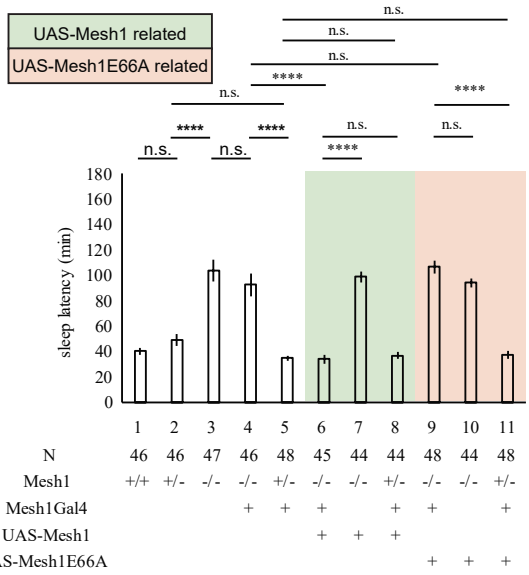

	1	2	3	4	5	6	7	8	9	10	11
N	46	46	47	46	48	45	44	44	48	44	48
Mesh1	+/+	+/-	-/-	-/-	+/-	-/-	-/-	+/-	-/-	-/-	+/-
Mesh1Gal4				+	+	+		+	+		+
UAS-Mesh1						+	+	+			
UAS-Mesh1E66A									+	+	+

C

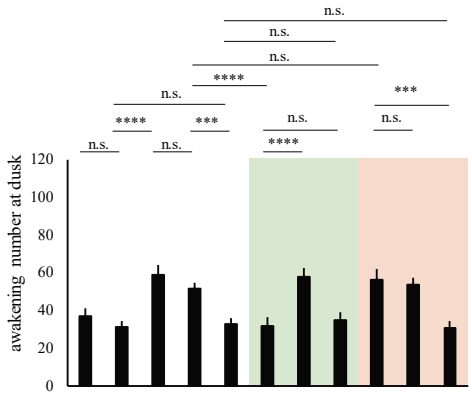

	1	2	3	4	5	6	7	8	9	10	11
N	46	46	47	46	48	45	44	44	48	44	48
Mesh1	+/+	+/-	-/-	-/-	+/-	-/-	-/-	+/-	-/-	-/-	+/-
Mesh1Gal4				+	+	+		+	+		+
UAS-Mesh1						+	+	+			
UAS-Mesh1E66A									+	+	+

D

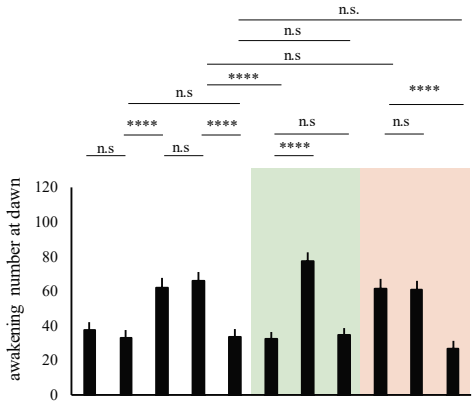

	1	2	3	4	5	6	7	8	9	10	11
N	46	46	47	46	48	45	44	44	48	44	48
Mesh1	+/+	+/-	-/-	-/-	+/-	-/-	-/-	+/-	-/-	-/-	+/-
Mesh1Gal4				+	+	+		+	+		+
UAS-Mesh1						+	+	+			
UAS-Mesh1E66A									+	+	+

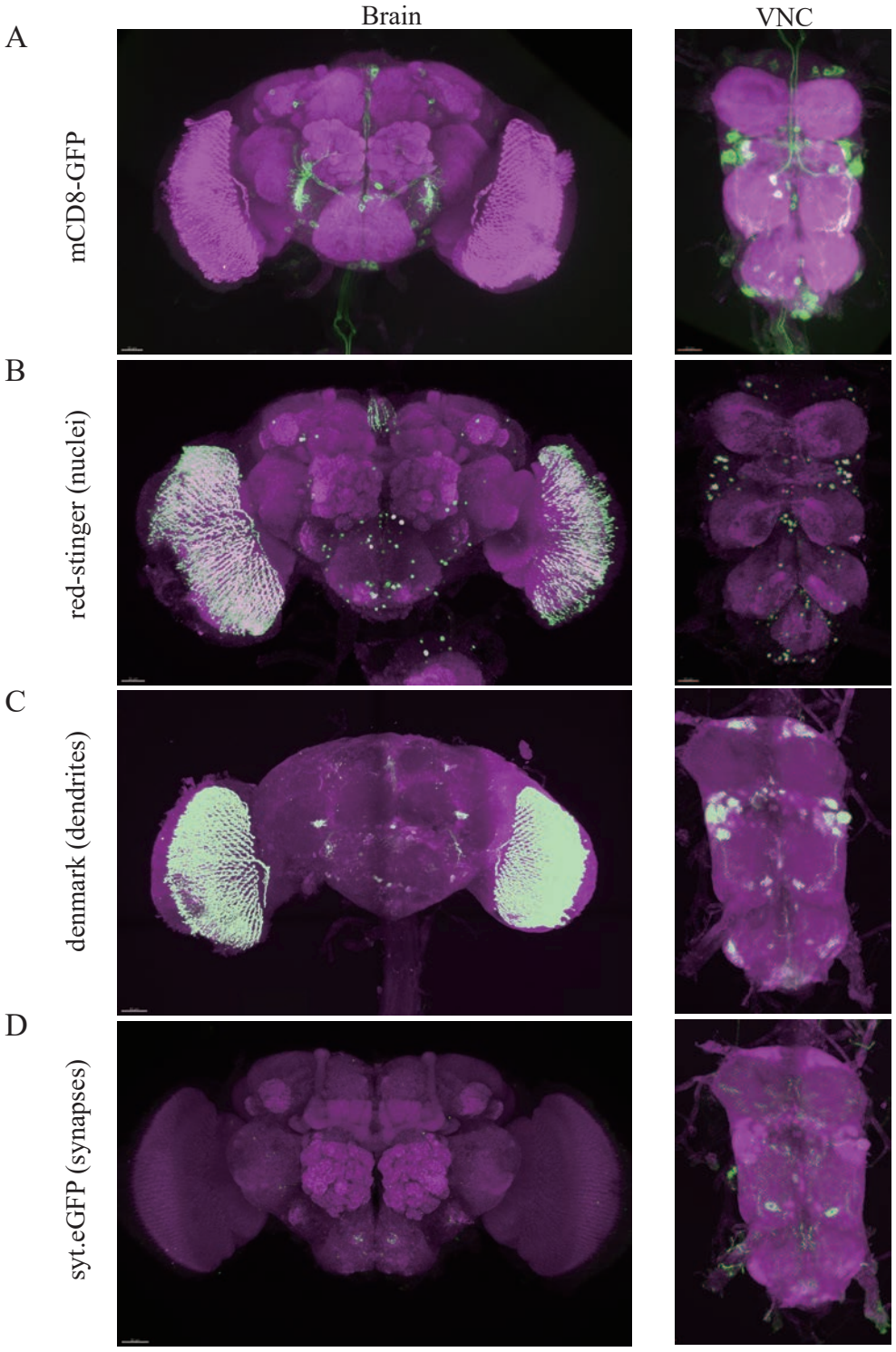

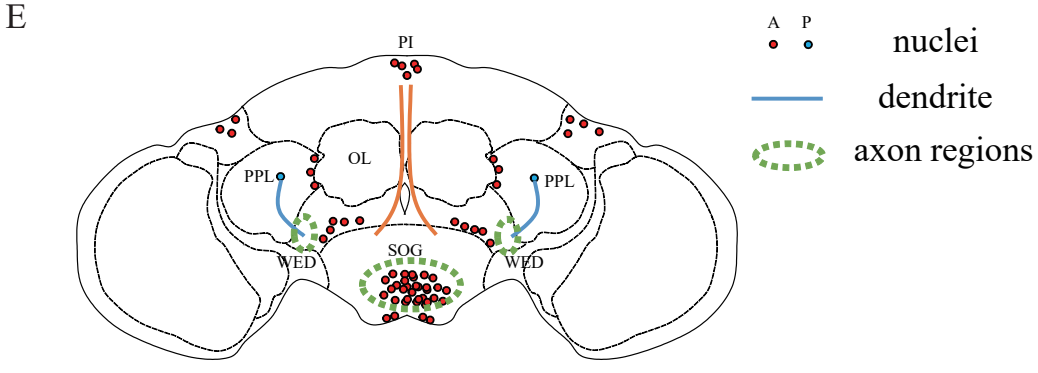

A

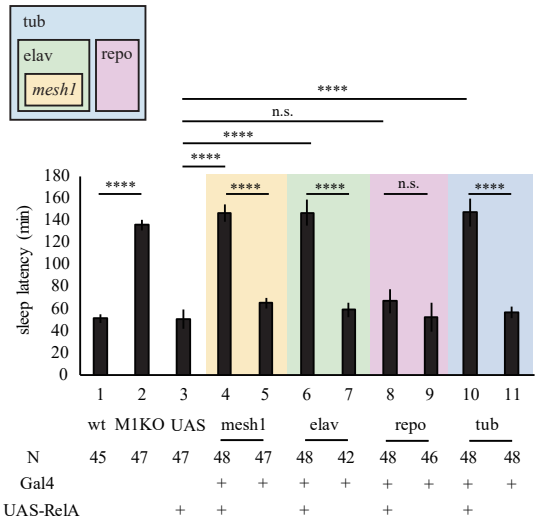

C

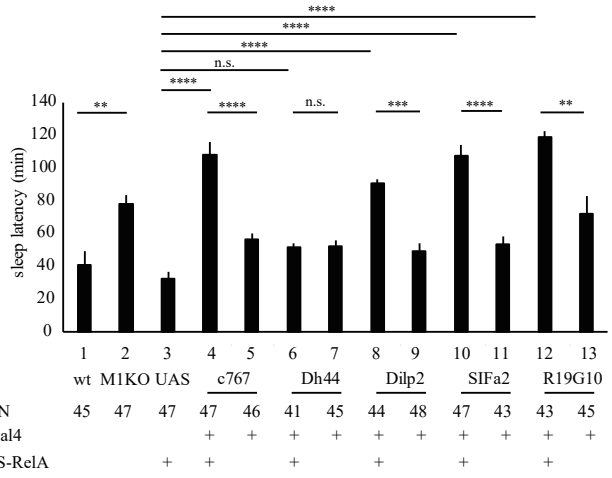

B

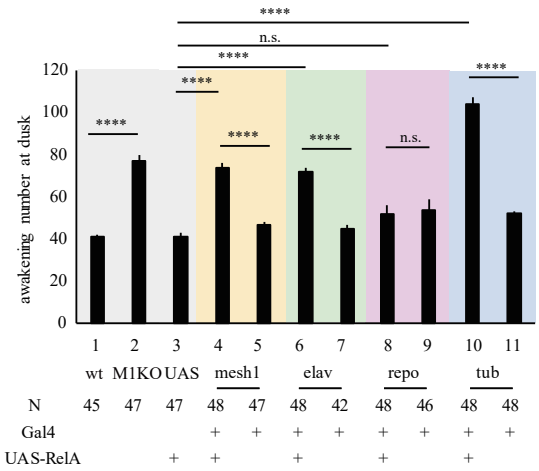

D

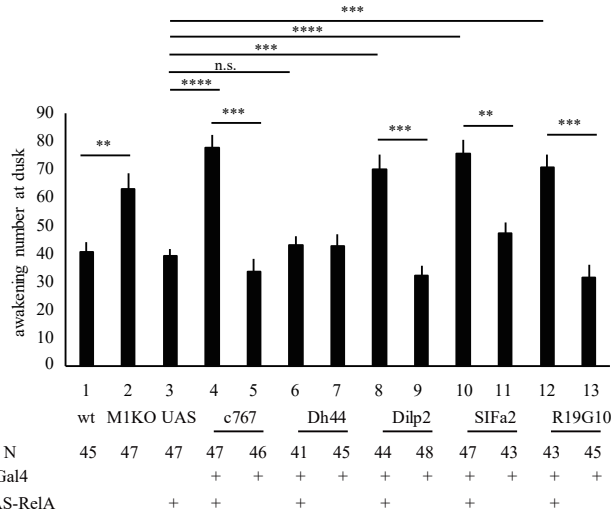

A

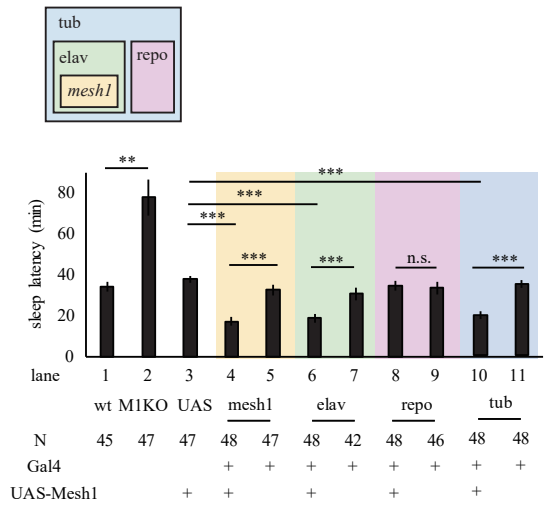

B

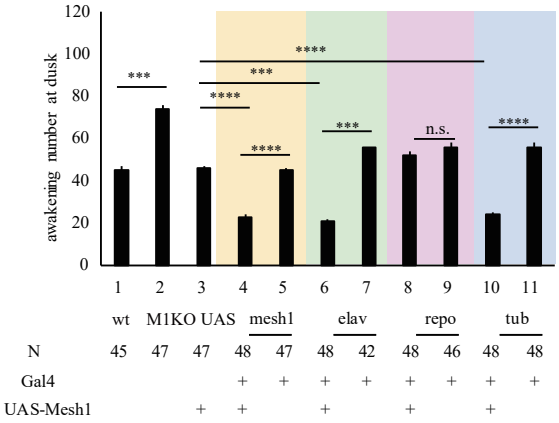

C

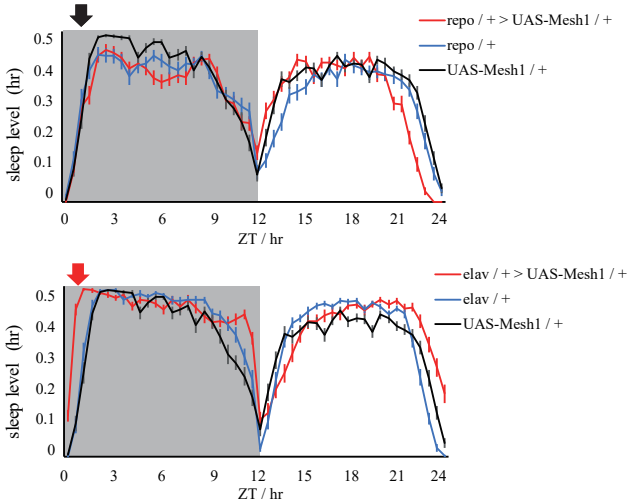

D

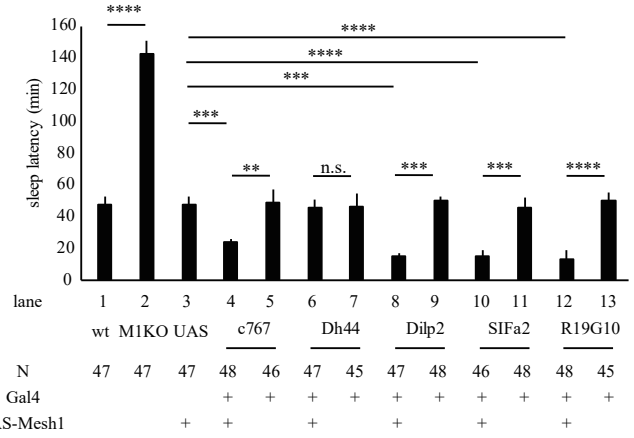

E

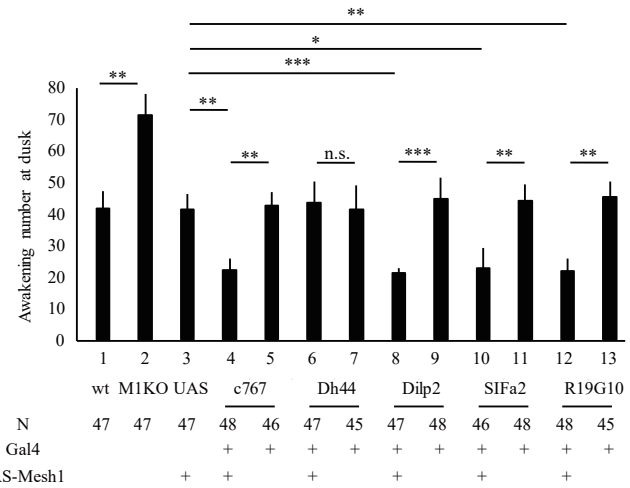

F

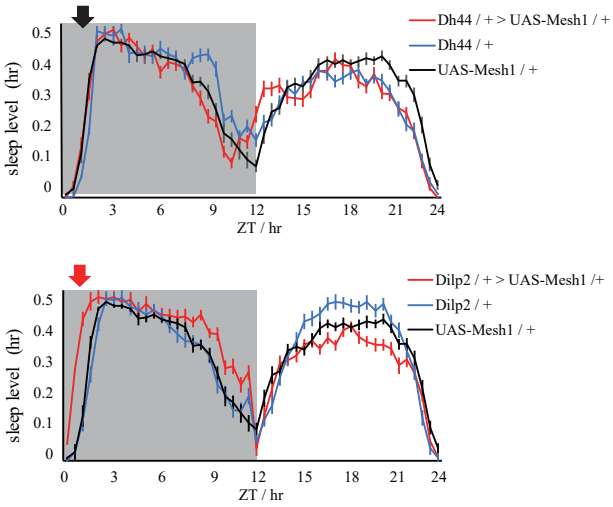

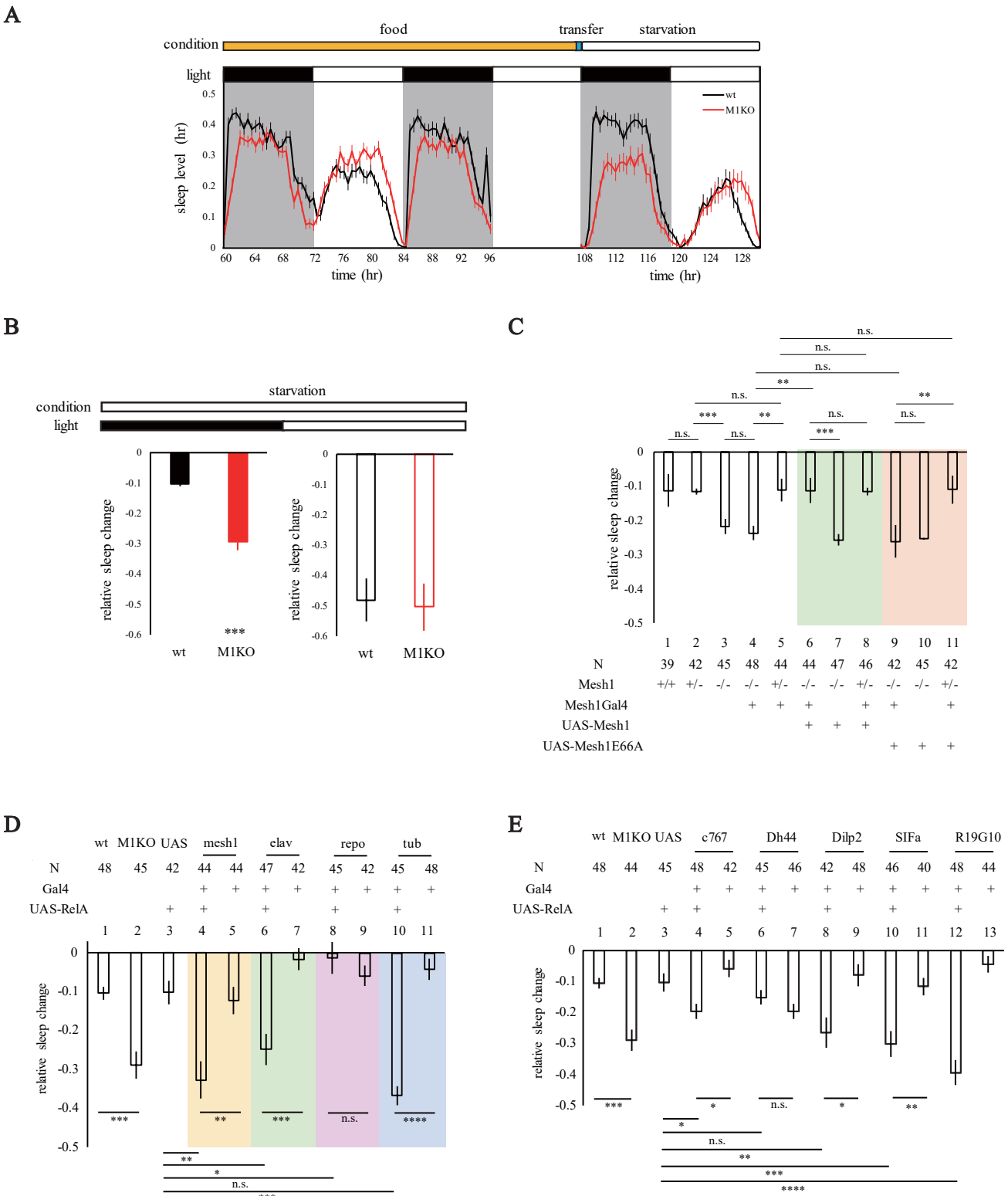

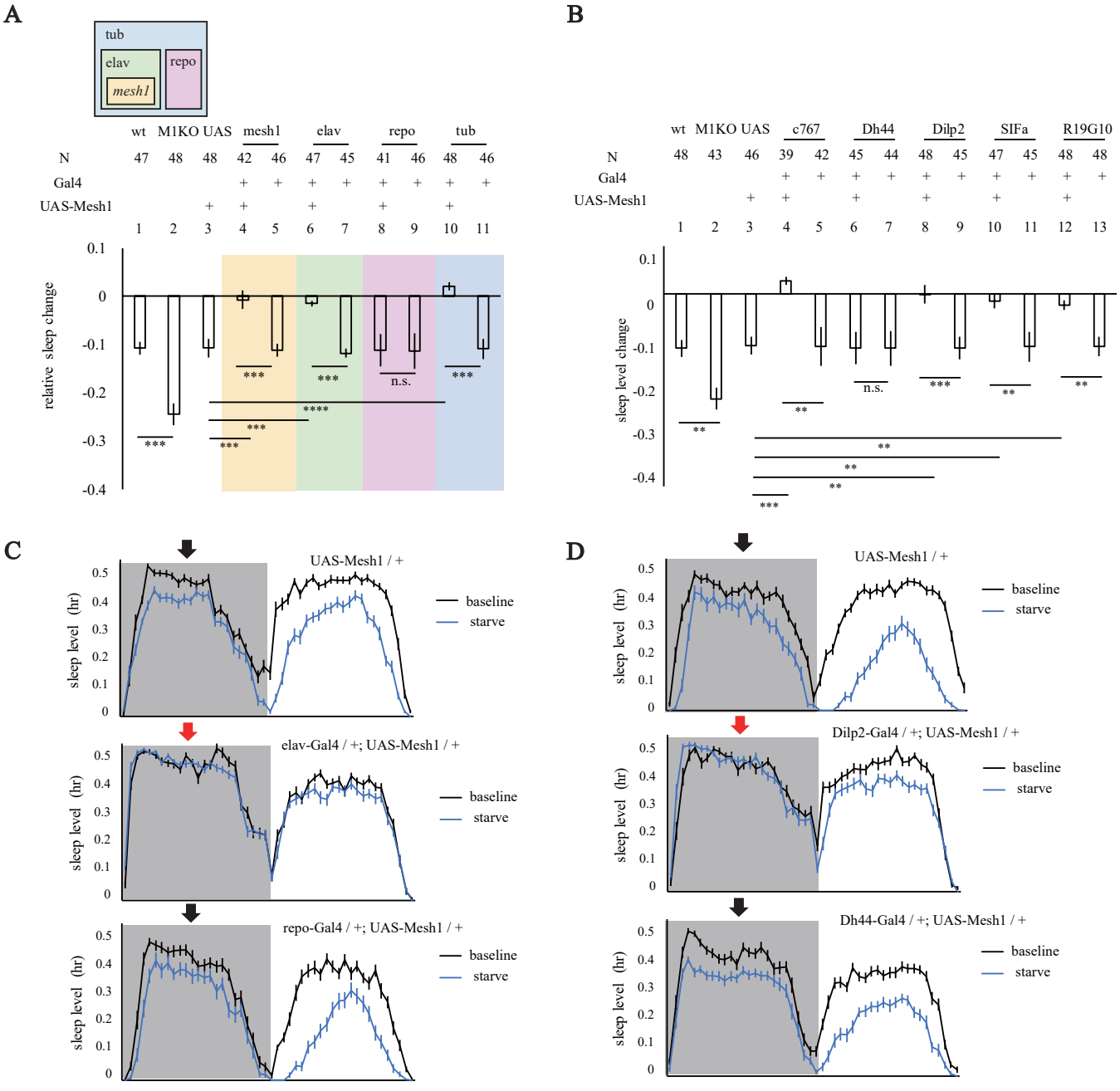

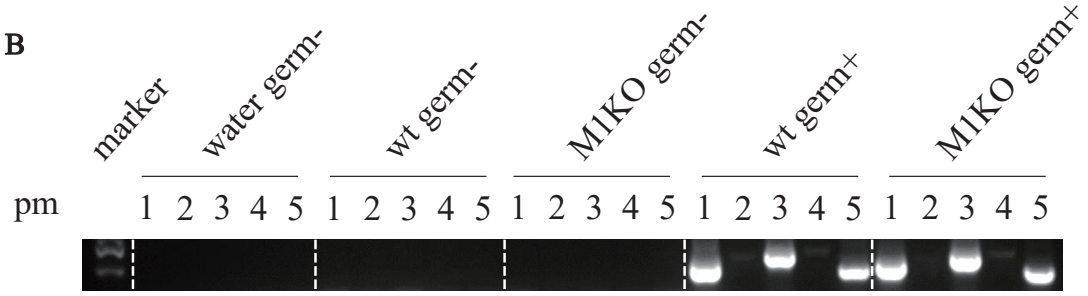

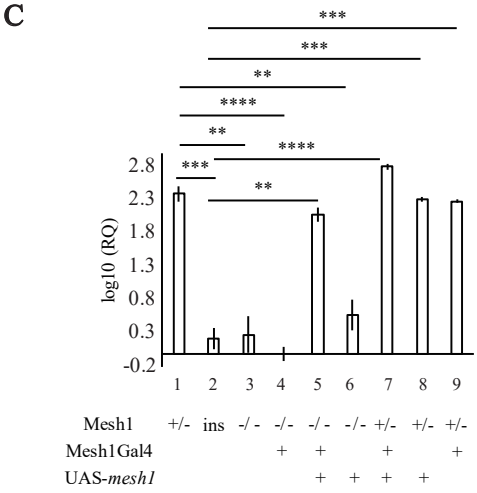

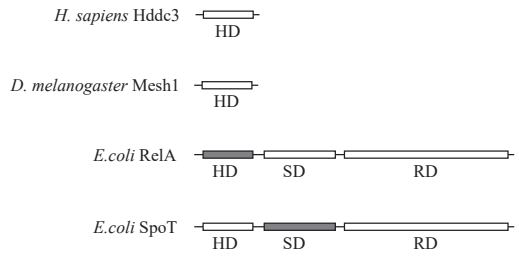

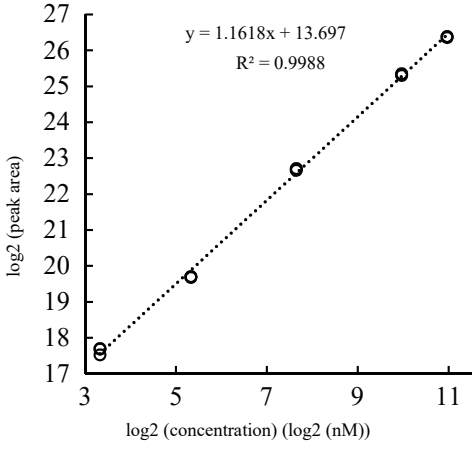

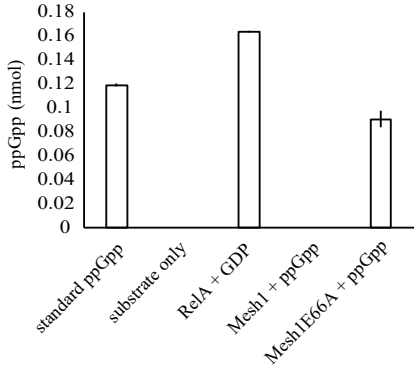

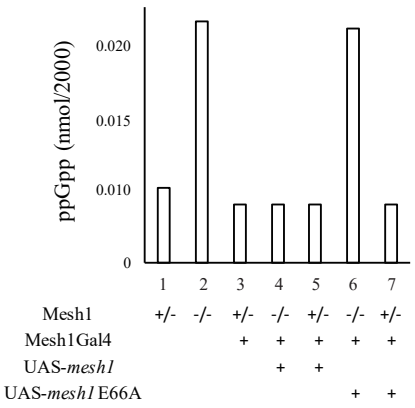

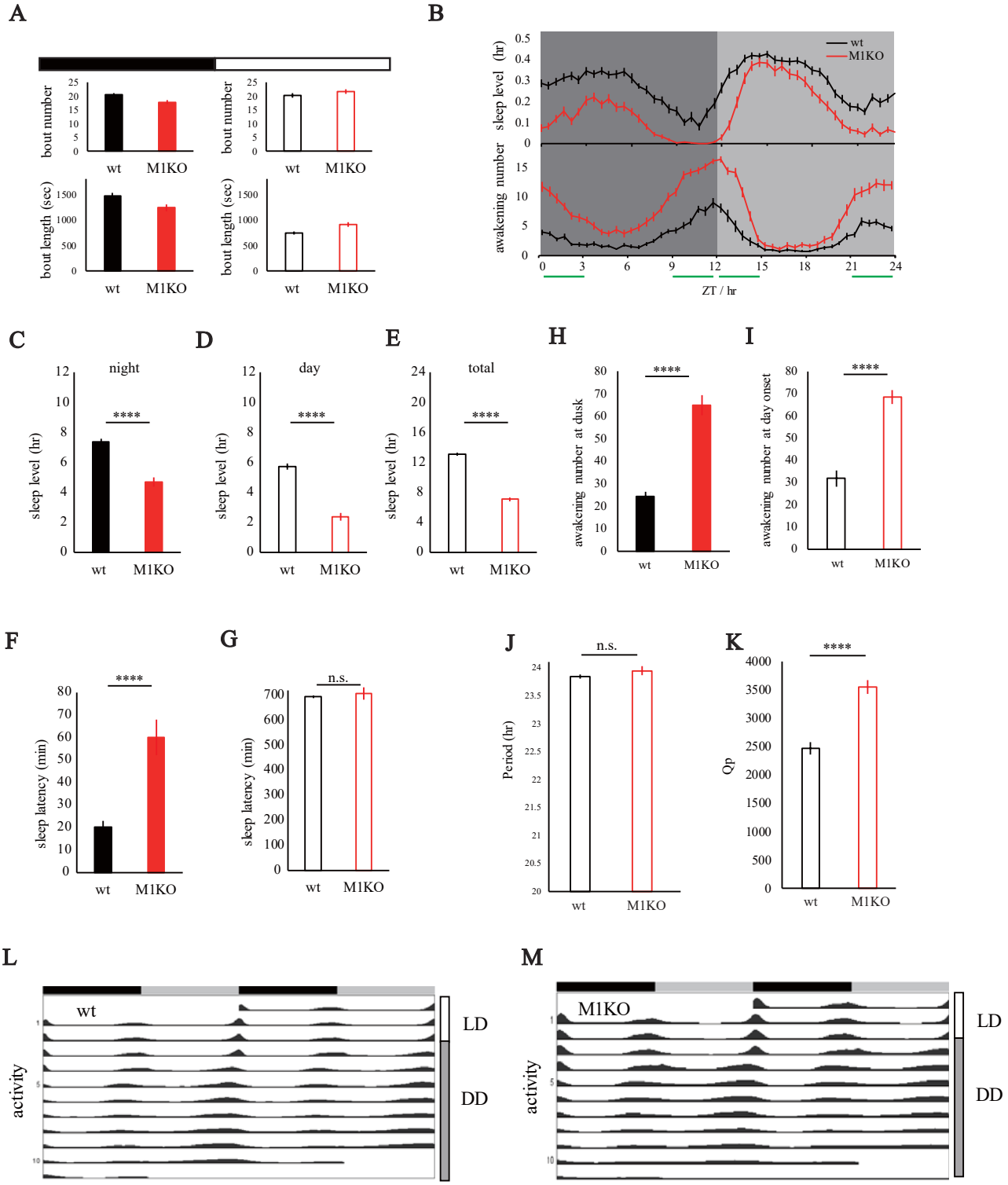

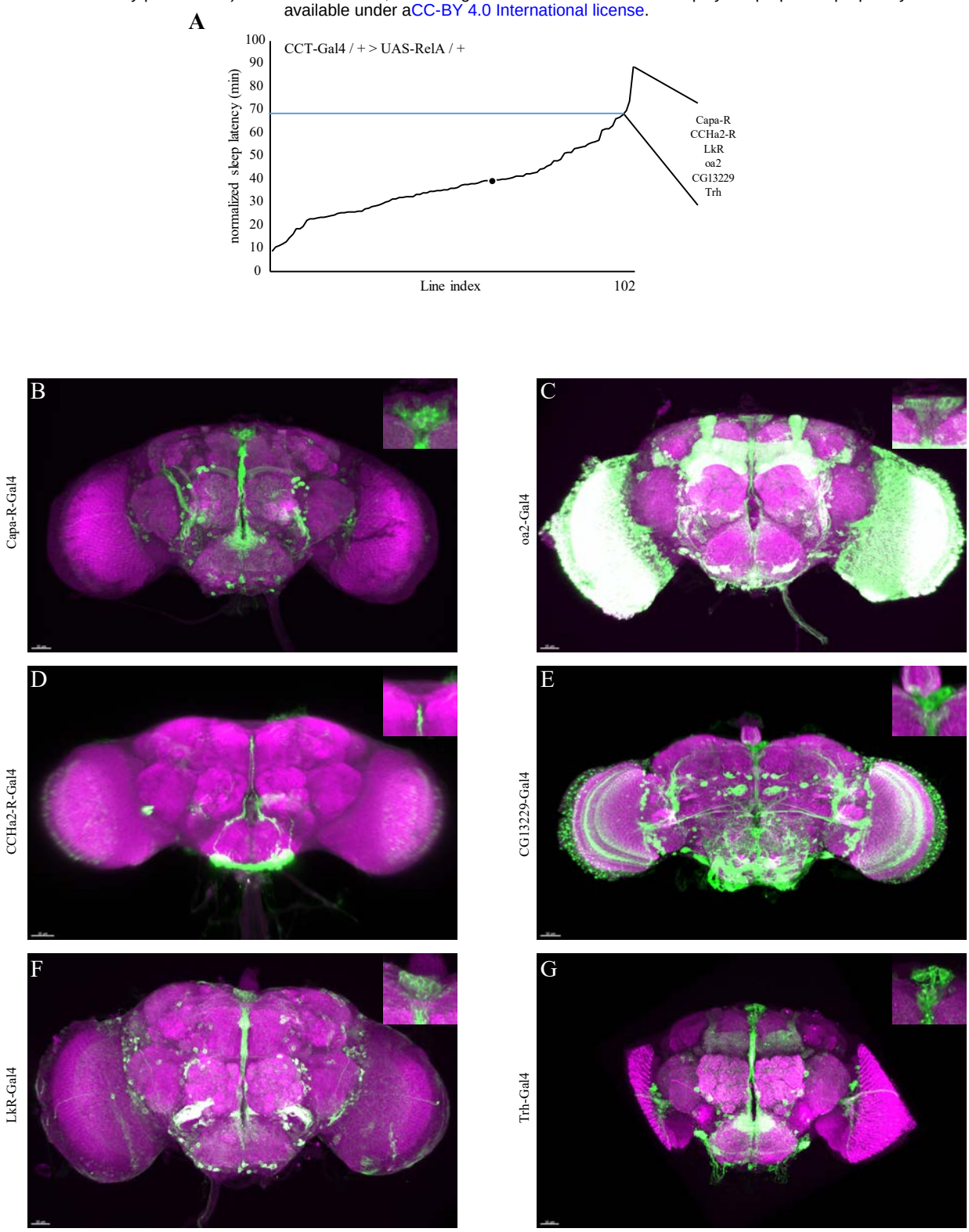

A

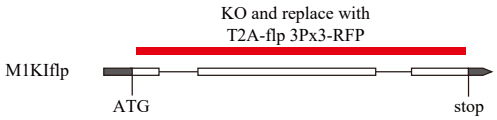

B

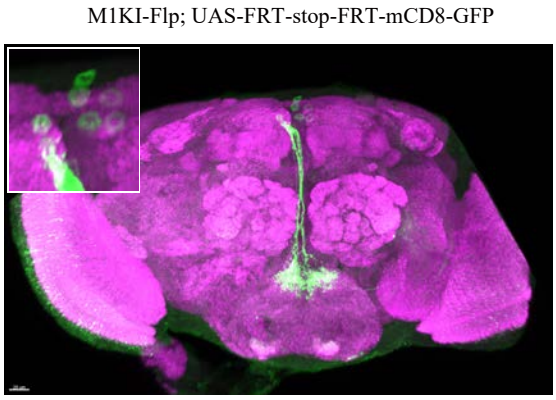

C

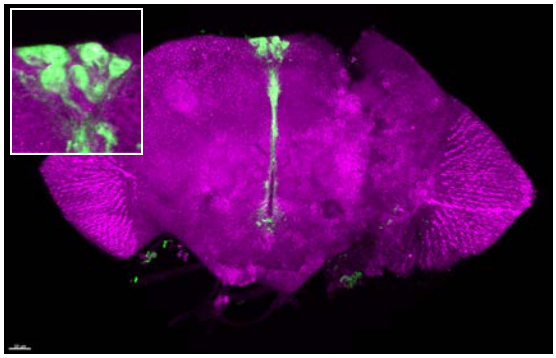

D

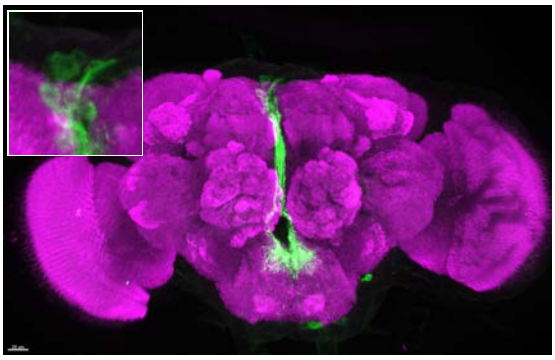

E